

AEROTHERMODYNAMIC MODELING AND SIMULATION OF GAS
TURBINES FOR TRANSIENT OPERATING CONDITIONS

A THESIS SUBMITTED TO
THE GRADUATE SCHOOL OF NATURAL AND APPLIED SCIENCES
OF
MIDDLE EAST TECHNICAL UNIVERSITY

BY

GÜLRU KOÇER

IN PARTIAL FULFILLMENT OF THE REQUIREMENTS
FOR
THE DEGREE OF MASTER OF SCIENCE
IN
AEROSPACE ENGINEERING

JUNE 2008

Approval of the thesis:

**AEROTHERMODYNAMIC MODELING AND SIMULATION OF
GAS TURBINES FOR TRANSIENT OPERATING CONDITIONS**

submitted by **GÜLRU KOÇER** in partial fulfillment of the requirements for
the degree of **Master of Science in Aerospace Engineering Department,**
Middle East Technical University by,

Prof. Dr. Canan Özgen _____
Dean, Graduate School of **Natural and Applied Sciences**

Prof. Dr. İsmail Hakkı Tuncer _____
Head of Department, **Aerospace Engineering**

Assist.Prof. Dr. Oğuz Uzol _____
Supervisor, **Department of Aerospace Engineering,**
METU

Dr. İlkey Yavrucuk _____
Co-supervisor, **Department of Aerospace Engineering,**
METU

Examining Committee Members:

Prof. Dr. Sinan Akmandor _____
Department of Aerospace Engineering, METU

Assist.Prof. Dr. Oğuz Uzol _____
Department of Aerospace Engineering, METU

Prof. Dr. Yusuf Özyörük _____
Department of Aerospace Engineering, METU

Dr. İlkey Yavrucuk _____
Department of Aerospace Engineering, METU

Assist.Prof. Dr. Sıtkı Uslu _____
Department of Mechanical Engineering, TOBB
University of Economics and Technology

Date: _____

I hereby declare that all information in this document has been obtained and presented in accordance with academic rules and ethical conduct. I also declare that, as required by these rules and conduct, I have fully cited and referenced all material and results that are not original to this work.

Name, Last Name: GÜLRU KOÇER

Signature :

ABSTRACT

AEROTHERMODYNAMIC MODELING AND SIMULATION OF GAS TURBINES FOR TRANSIENT OPERATING CONDITIONS

Koçer, Gülru

M.S., Department of Aerospace Engineering

Supervisor : Assist.Prof. Dr. Oğuz Uzol

Co-Supervisor : Dr. İlkey Yavrucuk

June 2008, 74 pages

In this thesis, development of a generic transient aero-thermal gas turbine model is presented. A simulation code, gtSIM is developed based on an algorithm which is composed of a set of differential equations and a set of non-linear algebraic equations representing each gas turbine engine component. These equations are the governing equations which represents the aero-thermodynamic process of the each engine component and they are solved according to a specific solving sequence which is defined in the simulation code algorithm. At each time step, ordinary differential equations are integrated by a first-order Euler scheme and a set of algebraic equations are solved by forward substitution. The numerical solution process lasts until the end of pre-defined simulation time. The objective of the work is to simulate the critical transient scenarios for different types of gas turbine engines at off-design conditions. Different critical transient scenarios are simulated for two different types of gas turbine engine. As a first simulation, a sample critical transient scenario is simulated for a small turbojet engine. As a second simulation, a hot gas ingestion scenario is simulated for a turbo shaft

engine. A simple proportional control algorithm is also incorporated into the simulation code, which acts as a simple speed governor in turboshaft simulations. For both cases, the responses of relevant engine parameters are plotted and results are presented. Simulation results show that the code has the potential to correctly capture the transient response of a gas turbine engine under different operating conditions. The code can also be used for developing engine control algorithms as well as health monitoring systems and it can be integrated to various flight vehicle dynamic simulation codes.

Keywords: generic gas turbine model, aero-thermal model, critical transients, off-design conditions, hot gas ingestion

ÖZ

GEÇİŞ KOŞULLARI ALTINDA ÇALIŞAN GAZ TÜRBİN MOTORLARININ AEROTHERMODİNAMİK MODELLEMESİ VE SİMÜLASYONU

Koçer, Gülru

Yüksek Lisans, Havacılık ve Uzay Mühendisliği Bölümü

Tez Yöneticisi : Yrd. Doç. Dr.Oğuz Uzol

Ortak Tez Yöneticisi : Dr. İlkey Yavrucuk

Haziran 2008, 74 sayfa

Bu araştırmada, jenerik bir gaz türbin motor modelinin geliştirilmesine yönelik bir çalışma sunulmaktadır. Herbiri gaz türbin motorunun bir bileşenini temsil eden, diferansiyel ve doğrusal-olmayan-cebirsal denklemler içeren bir simülasyon kodu geliştirilmiştir. Bu denklemler, her bir motor komponentinde gerçekleşen aerotermal süreçleri temsil eden denklemlerdir ve bu denklemler simülasyon kodunun algoritmasında belirli bir sıra takip edilerek çözülürler. Her zaman adımında, diferansiyel denklemler, birinci derece Euler tekniğiyle, doğrusal olmayan cebirsal denklemler ise ileri doğru yer değiştirme tekniğiyle çözülmüşlerdir. Nümerik çözüm süreci, daha önceden tanımlanan simülasyon süresi bitiminde sona erer. Yapılan çalışmanın amacı, tasarım noktası dışındaki noktalarda farklı gaz türbin motorları için kritik geçiş koşullarını simüle edebilmektir. İki farklı motor için farklı kritik senaryolar simüle edilmiştir. Birinci simülasyonda, küçük bir turbojet motoru için örnek bir kritik geçiş koşulu senaryosu, ikinci simülasyonda ise bir turboşaft motoru için sıcak gaz girişi senaryosu simüle edilmiştir. Ayrıca koda basit bir doğru orantılı kontrol algoritması da eklenmiştir.

İki simülasyon çalışmasında da ilgili motor parametrelerinin grafikleri çizilmiş ve sonuçlar sunulmuştur. Simülasyon sonuçları, geliştirilen simülasyon kodunun bir gaz türbin motorunun geçiş koşullarındaki davranışlarını simüle edebilme potansiyelinin olduğunu göstermiştir. Buna ek olarak kod, motor kontrol algoritmaları ve motor durumu izleme sistemleri geliştirme çalışmalarında kullanılabilir ve farklı hava aracı dinamik simülasyon kodlarına entegre edilebilir.

Anahtar Kelimeler: jenerik gaz türbin motor modeli, aero-termal model, simülasyon kodu, sıcak gaz girişi, kontrol algoritması

Babama ve anneme...

ACKNOWLEDGMENTS

I would like to express my gratitude to my thesis supervisor Asst.Prof. Dr. Oğuz Uzol and co-supervisor Dr. İlkey Yavrucuk for their guidance, advice, criticism, encouragements and insight throughout the research.

I would also like to thank Bora Yazıcı for his great support in performing experiments with SimJeT and Halil Kaya, Kemal Uçan, Ufuk Başlamışlı, Yılmaz Koç for their work on obtaining the calibration curve of SimJet.

Special thanks to my mother and father for their endless love and great support through out my studies and my career.

TABLE OF CONTENTS

ABSTRACT	iv
ÖZ	vi
DEDICATION	viii
ACKNOWLEDGMENTS	ix
TABLE OF CONTENTS	x
LIST OF TABLES	xii
LIST OF FIGURES	xiii
LIST OF ABBREVIATIONS	xvii
CHAPTERS	
1 INTRODUCTION	1
1.1 Background	1
1.2 Gas Turbine Engine Models	1
1.3 Gas Turbine Engine Modeling Applications	5
1.4 Objectives	8
1.4.1 Current Study	8
1.4.2 Outline	9
2 AERO-THERMAL TRANSIENT PERFORMANCE MODEL	11
2.1 Real Time Aerothermal Transient Performance Model	11
2.2 Structuring the Generic Aero-thermal Model	14
2.3 Reading The Compressor Map	20
3 SINGLE SPOOL TURBOJET SIMULATIONS	23
3.1 Turbojet Engine Characteristics	23
3.2 Results	25

4	COMPARISON OF SINGLE SPOOL TURBOJET ENGINE SIMULATIONS WITH TEST DATA	41
4.1	Experimental Set-up	41
4.2	Experimental Methods	44
4.3	Experimental Results	46
4.4	Comparison of the Experimental Results with Simulation Results	47
5	TURBOSHAFT SIMULATIONS	54
5.1	Turboshaft Engine Characteristics	54
5.2	Results	60
5.3	A Sample RPM Controller	67
6	CONCLUSIONS AND FUTURE WORK	70
6.1	CONCLUSIONS	70
6.2	FUTURE WORK	72
	REFERENCES	73

LIST OF TABLES

TABLES

Table 4.1	Specifications of the SimJet turbojet engine.	42
Table 5.1	Specifications of T800-LHT-800 turboshaft engine [17].	57

LIST OF FIGURES

FIGURES

Figure 2.1 Components and station numbers for real time aero-thermal transient performance model of two spool turbojet engine	12
Figure 2.2 Flowchart of aero thermal real time transient model for two spool turbojet-volumes method	13
Figure 2.3 Turbojet engine station numbering used in the aerothermal model.	15
Figure 2.4 Turboshaft engine station numbering used in the aerothermal model.	15
Figure 2.5 Flowchart for the generic aero-thermal gas turbine engine model, gtSIM.	16
Figure 2.6 Representation of beta lines grid generation.	21
Figure 2.7 Look-up tables data structure produced using the digitized compressor map.	22
Figure 3.1 A typical compressor map for a small turbojet engine as given in [5].	23
Figure 3.2 The digitized version of the compressor map given in Figure 3.1, which is used to generate the look-up tables.	24
Figure 3.3 The response of small turbojet engine rotational speed to step inputs in the fuel mass flow rate. Turbojet engine simulation scenario 1.	26
Figure 3.4 The response of small turbojet engine turbine inlet temperature to step inputs in the fuel mass flow rate. Turbojet engine simulation scenario 1.	27

Figure 3.5 The response of small turbojet engine thrust to step inputs in the fuel mass flow rate. Turbojet engine simulation scenario 1. . . .	28
Figure 3.6 The response of small turbojet engine rotational speed to linear increase and decrease in the fuel mass flow rate. Turbojet engine simulation scenario 2.	29
Figure 3.7 The response of small turbojet engine turbine inlet temperature to linear increase and decrease in the fuel mass flow rate. Turbojet engine simulation scenario 2.	30
Figure 3.8 The response of small turbojet engine thrust to linear increase and decrease in the fuel mass flow rate. Turbojet engine simulation scenario 2.	31
Figure 3.9 Engine moment of inertia term versus lag of engine rotational speed in time.	32
Figure 3.10 The response of small turbojet engine rotational speed to step inputs in the fuel mass flow rate. Turbojet engine simulation scenario 1 with the new engine inertia term.	33
Figure 3.11 The response of small turbojet engine turbine inlet temperature to step inputs in the fuel mass flow rate. Turbojet engine simulation scenario 1 with the new engine inertia term.	34
Figure 3.12 The response of small turbojet engine thrust to step inputs in the fuel mass flow rate. Turbojet engine simulation scenario 1 with the new engine inertia term.	35
Figure 3.13 The response of small turbojet engine rotational speed to linear increase and decrease in the fuel mass flow rate. Turbojet engine simulation scenario 2 with the new engine inertia term.	37
Figure 3.14 The response of small turbojet engine turbine inlet temperature to linear increase and decrease in the fuel mass flow rate. Turbojet engine simulation scenario 2 with the new engine inertia term.	38
Figure 3.15 The response of small turbojet engine thrust to linear increase and decrease in the fuel mass flow rate. Turbojet engine simulation scenario 2 with the new engine inertia term.	39

Figure 4.1	Small turbojet engine test setup.	43
Figure 4.2	Data Acquisition Control Panel used in the turbojet experiments.	45
Figure 4.3	Fuel Pump voltage versus fuel mass flow rate curve for the SIMJET Engine [21].	46
Figure 4.4	The response of engine rotational speed to quasi-step inputs in the fuel mass flow rate.	47
Figure 4.5	The response of engine thrust to quasi-step inputs in the fuel mass flow rate.	48
Figure 4.6	The response of engine exhaust gas temperature to quasi-step inputs in the fuel mass flow rate.	49
Figure 4.7	The response of engine model rotational speed to quasi-step inputs in the fuel mass flow rate.	50
Figure 4.8	The thrust response of the engine model to quasi-step inputs in the fuel mass flow rate.	51
Figure 4.9	The exhaust gas temperature response of the engine model to quasi-step inputs in the fuel mass flow rate.	53
Figure 5.1	T800-LHT-800 Turboshaft Engine.	55
Figure 5.2	Agusta A129 Mangusta Helicopter.	56
Figure 5.3	Compressor map of T800-LHT-800 as given in [17].	58
Figure 5.4	Digitized version of T800-LHT-800 compressor map that is used to generate the look-up tables.	59
Figure 5.5	The response of T800-LHT-800 engine gas generator speed to 5.3% and 15% increase in engine inlet temperature.	61
Figure 5.6	The response of T800-LHT-800 engine compressor pressure ratio to 5.3% and 15% increase in engine inlet temperature.	62
Figure 5.7	The response of T800-LHT-800 engine power output to 5.3% and 15% increase in engine inlet temperature.	64
Figure 5.8	Effect of HGI on the surge margin for two different inlet tem- perature distortions.	65

Figure 5.9 The response of T800-LHT-800 engine power output to double step input of temperature rise at engine inlet. Hot gas ingestion simulation scenario II.	66
Figure 5.10 The response of T800-LHT-800 engine gas generator speed with and without the control system.	68
Figure 5.11 The variation of the control parameter fuel flow rate.	69

LIST OF ABBREVIATIONS

<i>ECU</i>	Engine Control Unit
<i>HGI</i>	Hot Gas Ingestion
<i>LHV</i>	Lower Heating Value
<i>STOVL</i>	ShortTakeoffVerticalLanding
<i>VIGV</i>	Variable Inlet Guide Vane
<i>VTOL</i>	Vertical Take off Landing

LIST OF SYMBOLS

Π_c	compressor pressure ratio
η	efficiency
τ_{cc}	time constant
ω	angular speed
F	thrust
g_2	air mass flow rate at plenum exit
g_2'	air mass flow rate at compressor exit
g_3	air plus fuel mass flow rate at turbine inlet
g_c	Newton's constant
h	enthalpy
M_{cc}	mass accumulated in the combustor
N_{GG}	gas generator rotational speed
P_2	plenum exit pressure
P_2'	compressor exit pressure
P_c	compressor mechanical power
P_t	turbine mechanical power
P_{pt}	power turbine power
T_2	plenum exit temperature
T_2'	compressor exit temperature
T_3	turbine inlet temperature
T_4	turbine exit temperature

CHAPTER 1

INTRODUCTION

1.1 Background

A gas turbine extracts energy from a flow of hot gas produced by combustion of gas or liquid fuel in a stream of compressed air. It has an upstream air compressor (radial or axial flow) mechanically coupled to a downstream turbine and a combustion chamber in between. Energy is released when compressed air is mixed with fuel and ignited in the combustor. The resulting gases are directed over the turbine's blades, spinning the turbine, and mechanically powering the compressor. Finally, the gases are passed through a nozzle, generating additional thrust by accelerating the hot exhaust gases by expansion back to atmospheric pressure. Energy is extracted in the form of shaft power, compressed air and thrust, in any combination, and used to power aircraft, trains, ships, electrical generators, and even battle tanks.

1.2 Gas Turbine Engine Models

As being complicated systems, development and testing of gas turbine engines requires long time and large amount of money. After development phase, implementing control systems and health monitoring systems to maintain a safe operation for gas turbine engines requires additional cost which makes industry seek for a solution. As stated in [1] real-time gas turbine engine model can be used as a powerful tool in developing, testing and tuning control devices of gas

turbines. A high- fidelity computer model can be used to substitute a real engine for many applications such as:

- Rapid-prototyping of control or diagnostic systems;
- Verifying the functionality of mechanic and electronic devices;
- Reducing costs and time for control equipment setup.

Moreover, it can be possible to simulate critical transients that should be avoided on the actual plant due to risk of damage.

The practice of drawing trends from engine performance data in order to perform diagnostics studies has been around for a very long time. It is commonly known fact that engine condition monitoring is an effective but complex way to improve safety and reduce operation and maintenance costs of gas turbines. Increased competition amongst the civil airline industry and reduced budgetary allocations for the military have led to increased emphasis on reducing engine life cycle costs (LCC). The operation and maintenance of the propulsion system contributes substantially to the overall LCC. Engine health monitoring systems have become increasingly important in recent years due to the development of engines with improved power to weight ratios, the need to show enhanced reliability at reduced costs will require major advances in controls and diagnostics. Major advancements in computer technology and computational tools have brought a paradigm shift in the way the problem of diagnostics is being approached. In recent years there has been growing interest amongst research and user communities in the field of machinery prognostics, which is considered as the ultimate successor to diagnostics capability. The benefits of accurate engine diagnostics are related not only to the manufacturer, but also every user or maintainer throughout the chain of an engine life cycle. Increased competition within the civil airline industry has renewed interest towards reducing operating costs to improve profit margin.[2]

Gas turbine engine models are developed to perform simulations instead of running real gas turbine engines in order to reduce the cost of gas turbine engine control and health monitoring system development activities.

Real-time gas turbine engine simulations are essential for developing advanced and reliable engine control algorithms and health monitoring systems. They could also be used in increasing the fidelity of real-time flight simulators by integrating the engine simulation algorithms with the flight dynamics modeling and simulation codes. Predicting the off-design and transient behavior of gas turbine engines under various loading and operating conditions is of critical importance in order to ensure that the engine operates within safety limits and at optimum conditions.

As gas turbine controls become increasingly complex and development timescales get shorter, the need for systems to work right first time becomes more and more important. A major part of proving systems before they fly is by use of simulations which demonstrate the performance and safety features required. The use of simulation has become more important in developing systems in which the component elements interact in a sensible and safe manner.[3]

In order to simulate gas turbine engines, modeling of these engines are performed as a first step. As described in [4], there are various gas turbine engine models which can be structured for simulation purposes as follows:

- *Thermodynamic matching transient performance and control model*: This model comprises an engine thermodynamic model coupled to the digital control algorithms and subroutines to model the hydro-mechanical equipment. For this model there is no hardware unlike others described later. Main uses of this model are:
 - Design of engine control philosophy
 - Design of control schedules for fuel flow, VIGVs, variable area propelling nozzles, etc. to achieve engine transient requirements, while maintaining adequate surge and weak extinction margins
 - Examination of engine transient performance during the design phase, prior to an engine being available for transient testing.
 - Prediction of engine transient performance in extreme corners of the operational envelope where engine testing may not be practical. For

aero- engines, Airworthiness Authorities will accept such model data as proof of safety, once the model has been aligned to test data at more convenient operational conditions.

- Examination of manoeuvres which may be too expensive or impractical to test, such as shaft breakage.
- *Real time transient performance model:* These models are composed of a software combined with hardware control system. The hydro-mechanical systems are shown in hardware as well as the digital controller. This layout often referred to as a iron bird for aero applications, requires hydraulic pressure, electrical power, etc to be available so that all of the hydro-mechanical systems can be actuated. At earlier stages in a project these systems may be modelled in software with only the digital controller in hardware. These models are have a multitude of uses:
 - Development of the control hydro-mechanical hardware independent of an engine. This is a big cost saving , and also means that the control hardware can be tested early in the development programme before an engine is available.
 - Proving the machine code digital controller algorithms before utilising them on a real engine. Hence the machine code implementation of the control philosophy, designed using the matching model, can be validated to ensure that there are no translation errors which may have endangered an engine.
 - "Passing off" production control systems
 - Providing the engine model for flight simulators for training pilots.
 - Assessment of control system and overall stability, providing there is no iteration and consequent noise on output parameters.
- *Real time aerothermal transient performance model:* The aerothermal model is the most accurate of the many real time engine models for modelling engine performance transient parameters. Relative to matching model this method has superior execution time, as it does not require iteration, though there is some loss in accuracy. It is the most commonly used model

for engine control system hardware development, due to it being the most accurate real time engine model. The other model types described below are more suited to flight simulators, where lower accuracy is permissible.

- *Real time transfer function transient model:* In this type of real time engine model, key performance parameters are related to fuel flow using a transfer function equation. This model is generally less accurate than the aero thermal real time model, however it is simpler and faster. Although sometimes used for control system development it is more common in flight simulators. Here auxiliary system parameters such as for the oil or starter system are required in addition to engine performance parameters, and can easily be modeled in this way.
- *Real time lumped parameter transient performance model:* In this type of real time engine model a large matrix of steady state and transient performance parameters is generated from aero thermal models or test data. This model is again more suited to flight simulators but is not as commonly used as the transfer function method.

1.3 Gas Turbine Engine Modeling Applications

In previous work, non-linear aero-thermal models are developed on a basis of mathematical models which are composed of a set of differential equations plus a set of non-linear algebraic equations in a sequence (e.g. [5], [6], [1]). In these studies, aero-thermal models for various types of gas turbine engines are used to simulate real-time engine performance in order to either implement a control system to the engine or to monitor engine parameters for diagnostics. A novel high-fidelity real-time simulation code based on a lumped, non-linear representation of gas turbine components is presented by [6]. In this study, it is shown that the set of non-linear algebraic equations and ordinary differential equations that compose the mathematical model of the gas turbine can be solved by means of a forward substitution procedure. The code developed is based on the object-oriented approach and is realized under the Matlab-Simulink graphical environment: a library of blocks that simulate the gas turbine components are set

up and a description of main blocks are provided. According to the results of this study, the developed code is compatible with the software package called Real-Time-Workshop® toolbox. By means of this tool, a source code in C language is automatically generated from the Simulink model and can be compiled. This feature represents a chance useful to modify an existing code or to realize a new one in a relatively short time from models already tested in the Simulink environment. Two different gas turbines for power generation are simulated with a relatively high level of details. Some tests have been carried out on the programs obtained by compiling the C codes generated by means of the described procedure. Such tests showed that the codes are able to provide the results in real time, even using a simple personal computer. The source code in C language can be also modified in order to realize hardware-in-the-loop applications for testing control equipments or for control embedded applications or diagnostic purposes.

Some other mathematical models have also been developed in order to construct the simulation algorithm. A simplified mathematical model of twin shaft gas turbine engine suitable for use in dynamic studies of both electric power generation plants and variable speed mechanical drive applications has been presented by [7]. In this study, the development of a simplified parametric model, based on a lumped parameter approach and able to predict the off-design and the dynamic behaviour of twin-shaft gas turbines in a relatively large power range is introduced together with the comparison of performance prediction capabilities of the simplified model with a more detailed thermodynamic model in the transient behaviour simulation of a ship propulsion gas turbine plant. It is stated that the comparison between the predicted trends following changes in the fuel flow shows that the simplified model very closely approximates the dynamic response of the rigorous one.

In [8], a mathematical model for each component is developed using physical laws or empirical data when available. In this study, modeling, matching, and simulation of a gas turbine engine for power generation is presented. According to the results of the study,

- Matching conditions between the compressor and the turbine may be met by superimposing the turbine performance characteristics on the compressor performance characteristics with suitable transformation of the coordinates.
- Matching technique can be used to determine the following:
 - the operating range (envelope) and running line of the matched components
 - the proximity of the operating points to the compressor surge line
 - the maximum operating point at the maximum turbine inlet temperature
 - most importantly, (from the figures) whether the gas turbine engine is operating in a region of adequate compressor and turbine efficiencies
- The computer program written for simulating a gas turbine engine satisfies the matching conditions analytically between the various components to produce the equilibrium running line. Hence, it can serve as a very useful tool for simulating gas turbine engines. The principal advantages of the gas turbine simulation program are summarized as follows:
 - The computer simulation program can help in investigating the effects of the components performance characteristics on the performance of the complete engine. This investigation can be carried out at the design stage without bearing the cost of manufacturing and testing an expensive prototype.
 - The conceptual designs of the engine can be studied, and the choice of a particular concept can be made to suit the specified operational requirements.
 - The matching of the components can be explored for the design, off-design, and transient conditions.
 - The simulation program can serve as a valuable tool for investigating the performance of the gas turbine at off design conditions. This investigation can help in designing an efficient control system for the gas

turbine engine of a particular application, including being identical to the combined power and power (CPP) plant.

Instantaneous-response and transient-flow component models have been adapted for the prediction of the transient response of gas turbine cycles by [9]. In this study, the component models based on the transient form of the conservation of mass, energy, and momentum within each component are coupled to simulate a closed cycle regenerative gas-turbine cycle with components suitable as powering units of small space systems. During transients the cycle parameters of the overall system are iteratively evaluated. A converged solution for each time step is obtained by an iterative scheme based on the principle of conservation of working-fluid mass in the system. Various system transients are studied and it is concluded that the transient turbo-machinery models are required for higher-frequency transients, such as those that may be introduced by the engine control system.

In [5], development of simple real time transient performance model for jet engine control is presented. An quasilinear simple fast engine model is discussed in this study which has maximum accuracy for maximal variance of the fuel flow input command in accordance to the jet engine control system specifications. The fast model is obtained using the Novel Generalized Describing Function, proposed for investigation of nonlinear control systems. This function provides the investigation of periodic oscillations in a nonlinear closed-loop control system. The results of this study shows that, the novel model is meant to simplify controller design according to the control system specifications which declare the limiting parameters of maximal input response in transient operation.

1.4 Objectives

1.4.1 Current Study

In this thesis, development studies of a generic aero-thermal gas turbine engine model is presented. A simulation code is developed based on the real time

aero-thermal transient performance model and two different gas turbine engine simulations are performed.

In the first simulation study, in order to predict the off-design and transient behavior of a small turbojet engine under various loading and operating conditions, different fuel scheduling scenarios are simulated. An aero-thermal model of a small turbojet engine with no bleed and no turbine cooling is developed in order to simulate the critical transients that it may suffer at off-design operating conditions. The algorithm is composed of a set of differential equations and a set of non-linear algebraic equations representing each turbojet engine component. Results of the engine response are presented for two sample scenarios that simulates different fuel scheduling applications.

In the second simulation study, an aero-thermal model of T800-LHT-800 turboshaft engine with no bleed and no turbine cooling is developed in order to simulate the critical transients that it may suffer during various Hot Gas Ingestion (HGI) scenarios. In this simulation study, responses of various engine parameters such as gas generator speed, compressor pressure ratio and power available are presented for two different HGI scenarios. In addition, the engine responses to the temperature distortion at the inlet are presented when a simple control algorithm is implemented to keep the engine rpm constant, simulating the existence of a simple speed governor.

In the simulation studies, steady compressor maps are used in order to simulate the divergence of the engine response from the corresponding operating line for certain critical transient scenarios.

1.4.2 Outline

This thesis is composed of six chapters:

In chapter 2, the methodology and the details of the aero-thermal gas turbine engine model and the simulation code are presented.

In chapter 3, the results of the small turbojet engine simulation study are pre-

sented.

In chapter 4, a validation study performed by running a small turbojet engine in a test facility in order to measure the input fuel flow rate and responses of engine rotational speed, exit temperature and thrust of a small turbojet engine. The values from the same fuel flow rate scenario are inputted to the turbojet simulation code and the engine rotational speed, thrust and exhaust gas temperature response graphs of the small turbojet engine and the model are compared.

In chapter 5, simulation of T800-LHT-800 turboshaft engine including the critical transients that it may suffer during various Hot Gas Ingestion(HGI) scenarios are presented.

Finally, in chapter 6 the points which are concluded as a result of this study and future work are presented.

CHAPTER 2

AERO-THERMAL TRANSIENT PERFORMANCE MODEL

2.1 Real Time Aerothermal Transient Performance Model

The real time aerothermal transient performance model is the most accurate of the many real time engine models for modeling engine performance transient parameters. It is the most commonly used model for engine control system hardware development. The aero-thermal transient performance model developed as a part of this study is based on the algorithm given in Walsh and Fletcher[4]. A sample application of this algorithm to a two-spool turbojet engine as explained in [4] is also included here for completeness purposes. In this study, this algorithm and this specific application is further modified, revised and a generic aero-thermal gas turbine engine model is developed.

Figure 2.1 shows the component breakdown and station numbers employed for a two spool turbojet engine, while Figure 2.2 shows the computation procedure required. As per the matching model a steady state point is run and then the model switches to transient mode and runs points at intervals of time corresponding to the digital controller update time frame.

The volumes between the turbomachinery are important in the calculations. Figure 2.2 shows that after time has been incremented from time $t-1$ to time t , the first calculations are the computation of P26, P45 and P6 using values of dP/dt calculated from volume dynamics at the end of the previous point at

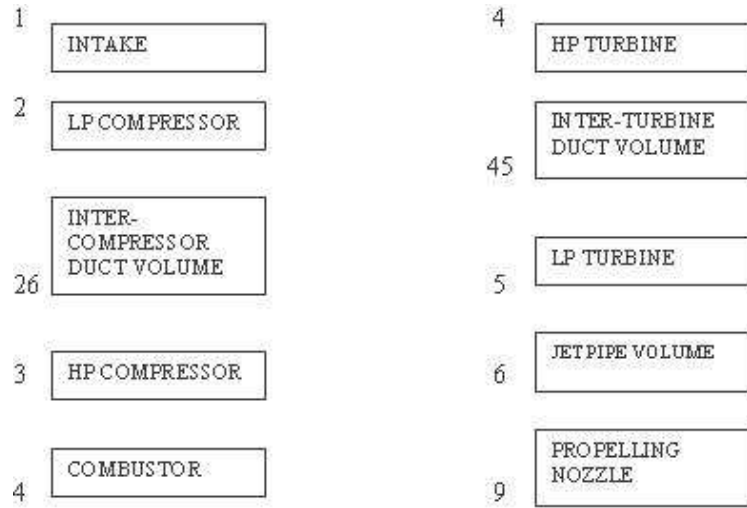


Figure 2.1: Components and station numbers for real time aero-thermal transient performance model of two spool turbojet engine

time $t-1$. Speeds at time t are now also calculated using unbalanced powers, speeds from the previous point and the spool inertias. The computation then moves to the combustor, calculating T_4, P_4 and P_3 using the fuel flow scheduled from the control system, and mass flows and temperatures from previous time step. Next in the HP turbine the component map as per the matching model is employed, but capacity and efficiency are looked up using the known expansion ratio and corrected speed. Hence T_{45} and W_4 are calculated. The computation then loops back through the combustor three times to update the W_4 used to time t as opposed to time $t-1$.

Next, intake calculations are performed as per steady state routines, and then the LP compressor map is read using the known pressure ratio and referred speed yielding W_2, W_{26} and T_{26} . This process is repeated for the HP compressor map to give T_3 and W_3 . The computation then loops back through the combustor three times to update W_3 and T_3 to values at time t as opposed to values at time $t-1$. If these loops slow the computation down unacceptably then they may be omitted with little loss of accuracy.

The LP turbine map is then read using the known expansion ratio and corrected speed, and hence T_6, W_{45} and W_5 are evaluated. The propelling nozzle capacity

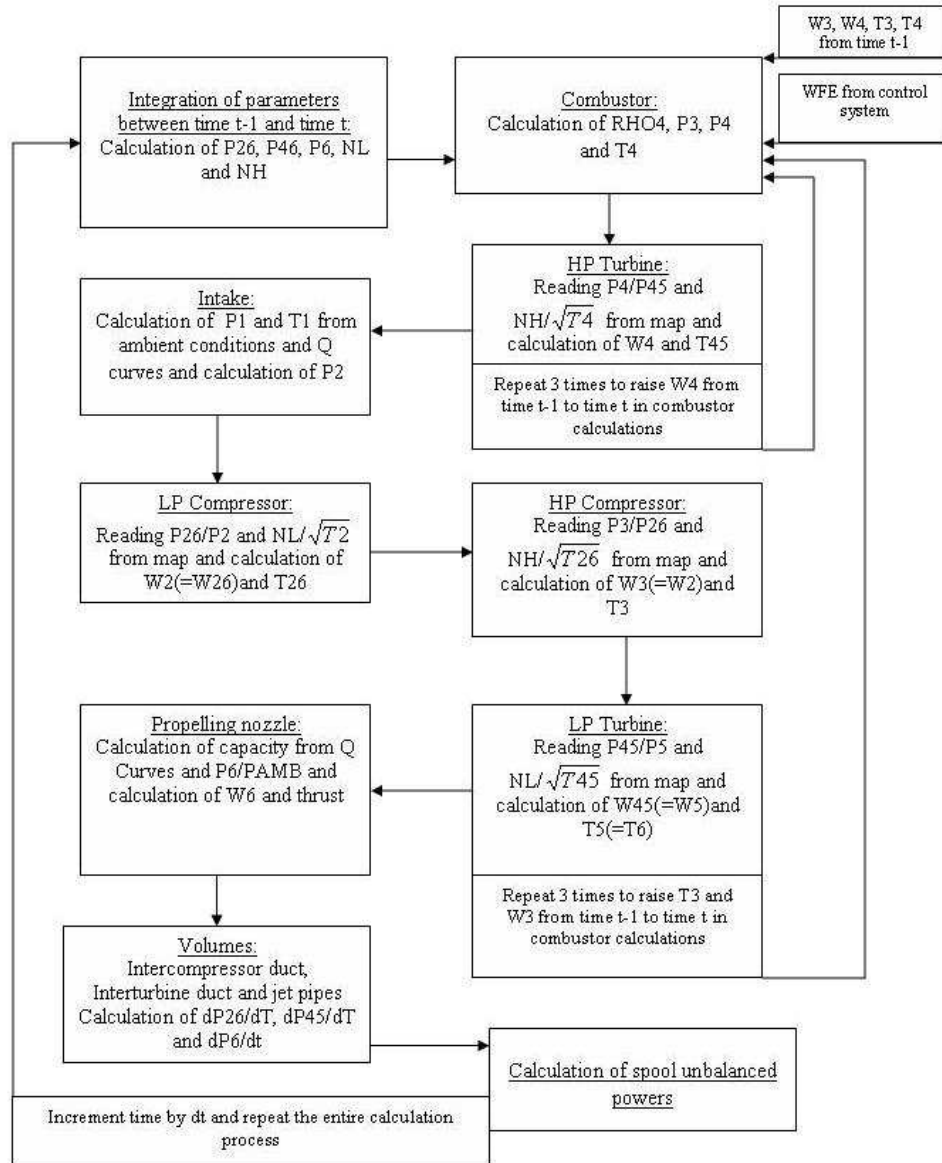


Figure 2.2: Flowchart of aero thermal real time transient model for two spool turbojet-volumes method

and hence $W6$ can then be calculated from its expansion ratio, effective area and Q curve formulae given in chapter 5 of [4]. The expansion ratio is $P6$ divided by ambient pressure, or the critical value if the nozzle is choked. For each of three inter-component volumes dP/dt is then calculated, using mass flows entering and leaving the volumes as calculated via above.

Finally the spool unbalanced powers are evaluated, after which time is incremented again for the next transient point. Relative to the matching model this method has superior execution time, as it does not require iteration, though there is some loss in accuracy.

2.2 Structuring the Generic Aero-thermal Model

The aerothermal gas turbine engine model which is developed in the current study is based on a mathematical model which consists of the governing equations representing the aero-thermodynamic process of the each engine component. Compressor and turbine are considered as volume-less elements and a capacity plenum is introduced at the outlet of the compressor in order to take into account the unsteady mass balance. Combustor is considered as a pure energy accumulator as described in [6]. Figure 2.3 and Figure 2.4 show the station numbering used in developing the simulation codes for turbojet and turboshaft engines separately. This numbering scheme is rather different than the typical schemes given in standard gas turbine related textbooks. However it's chosen to be consistent with previous studies in gas turbine simulations.

The simulation algorithm is given in Figure 2.5, and is the basis for the real-time simulation of both turbojet and turboshaft engines. In the simulation code, governing equations representing the aero-thermodynamic process of each engine component and the shaft dynamics are solved according to the solving sequence given in the figure above. At each time step, ordinary differential equations are integrated by a first-order Euler scheme and a set of algebraic equations are solved by forward substitution. As stated in [6], the computation

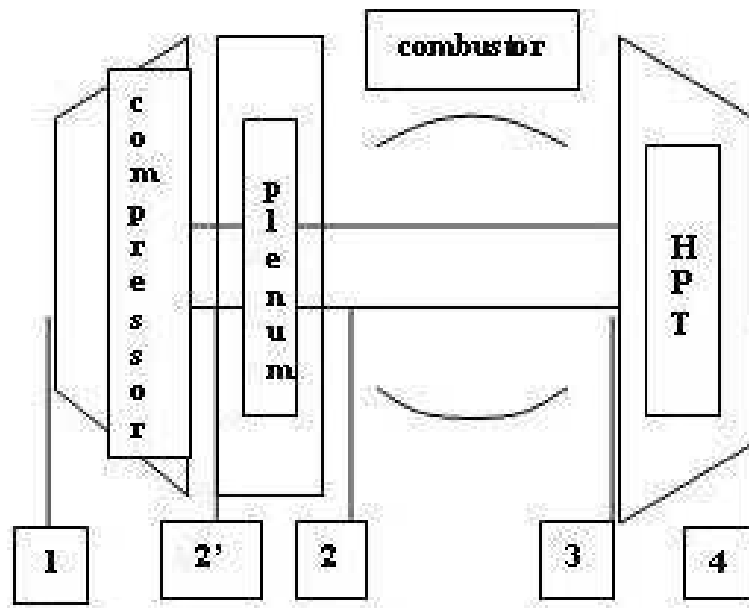


Figure 2.3: Turbojet engine station numbering used in the aerothermal model.

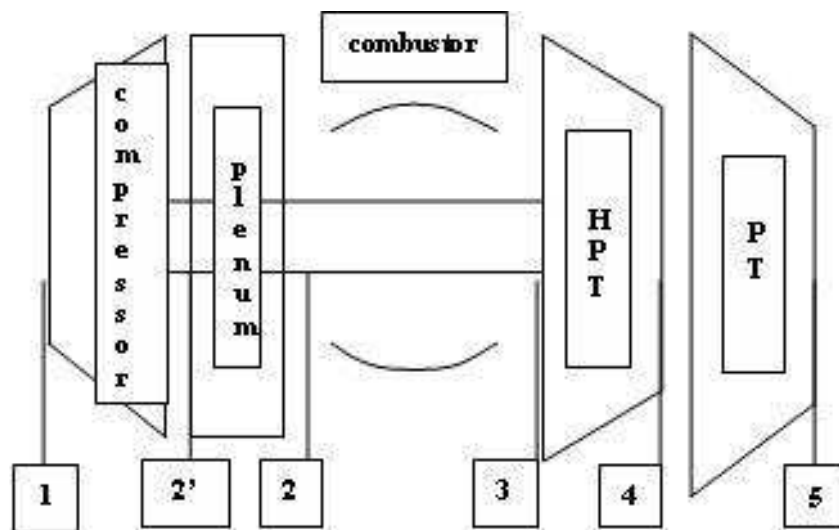


Figure 2.4: Turboshaft engine station numbering used in the aerothermal model.

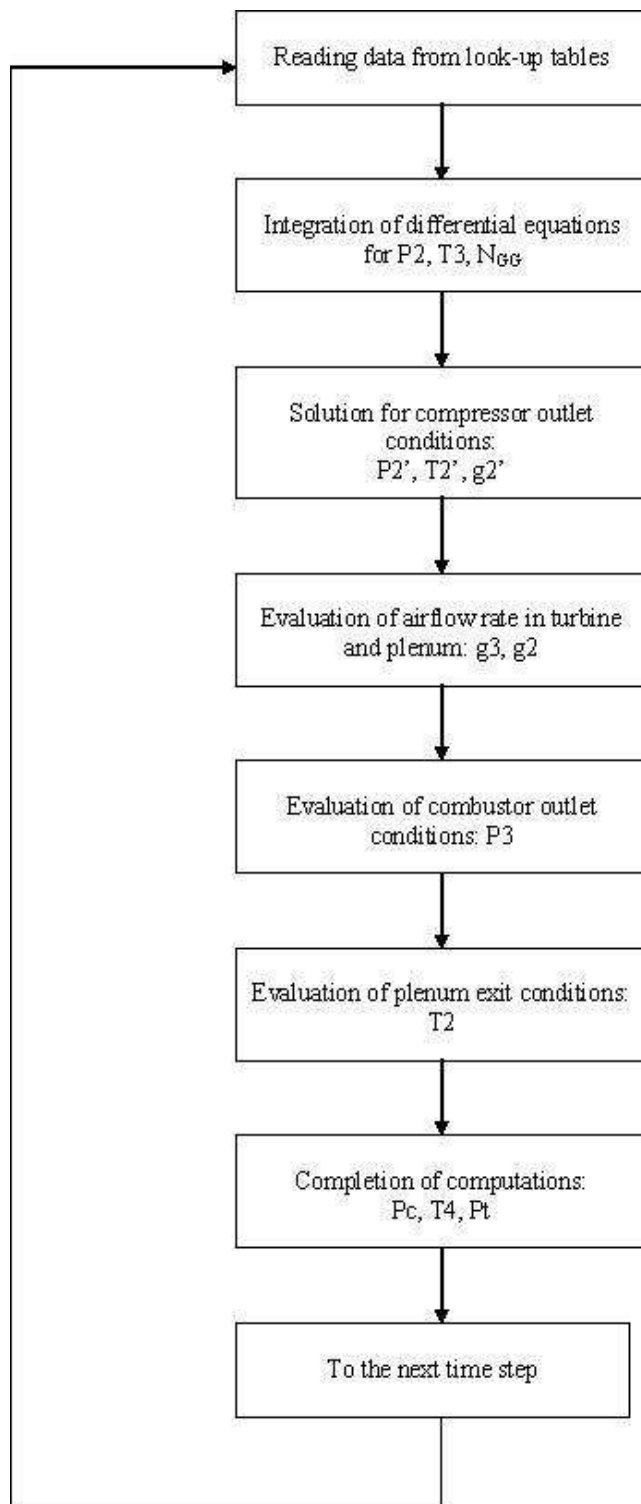


Figure 2.5: Flowchart for the generic aero-thermal gas turbine engine model, gtSIM.

results obtained by using a second order solver scheme confirmed that the small time step provides accurate solutions even using a first order scheme. It is also described in [6] that the results of the tests performed by using a previously developed simulation code which makes use of a fully implicit solving procedure show no discrepancies from the results obtained by using first and second order explicit schemes.

The shaft dynamics is represented by the angular momentum equation as:

$$\frac{d\omega}{dt} = \frac{1}{J \times \omega} (P_t - P_c - P_f). \quad (2.1)$$

where P_t represents the internal mechanical power of the turbine, P_c is the internal mechanical power required by the compressor and finally P_f represents a sum of power losses due to mechanical friction. J is the moment of inertia which includes the effects of the shaft and other connected devices.

Since the compressor is a volume-less element, unsteady mass balance is modeled through an adiabatic capacity called plenum. It is placed at the exit of the compressor. The flow speed inside the plenum is assumed to be constant. Temperature and pressure inside the plenum are supposed to vary with a polytropic law with exponent m . Unsteady mass balance is modeled through the adiabatic capacity "plenum" by applying the conservation of mass and represented by the following equation as:

$$\left(\frac{V_p}{m \times R \times T_{out}} \right) \times \left(\frac{dP_{out}}{dt} \right) = g_{in} - g_{out}. \quad (2.2)$$

where V_p is the volume of the plenum and the polytropic coefficient m is approximated by the specific heat ratio. The unsteady mass balance equation is used to calculate the pressure at the exit of the plenum to take into account the mass accumulation at the compressor exit during an engine transient. The turbines are assumed to be operating at choked flow conditions while modeling a twin spool gas turbine engine, the mass flow rate variations in between the two turbines is assumed to be minimal. Therefore a plenum was not added between

the two turbines. The choked flow concept through the turbines is applied by using a constant total pressure ratio values for each turbines.

As described in [6], the combustor is modeled as a pure energy accumulator by neglecting the mass balance which is taken into consideration at the upstream plenum block. Inside the combustor, temperature and pressure values are assumed to be homogeneous and equal to the combustor respective outlet values. The combustor is modeled by applying conservation of energy and represented as:

$$\tau_{cc} \times \frac{dT_{out}}{dt} = \frac{[g_{in} \times h_{in} + g_b \times (h_b + \eta_b \times LHV) - g_{out} \times h_{out}]}{g_{out} \times C_{p_{out}}}. \quad (2.3)$$

$$\tau_{cc} = \frac{M_{cc}}{k \times g_{out}}. \quad (2.4)$$

where M_{cc} is the mass inside the combustor, LHV is the lower heating value of the fuel, τ_{cc} is the time constant, h represents the specific enthalpy and η_b is combustor efficiency as given in [6]. The time constant, τ_{cc} is similar to an inertia term. For a bigger combustion chamber, M_{cc} term is larger meaning that it can hold large amount of air mass inside. Consequently a bigger combustor will respond to fuel addition slower compared to a smaller combustor. Therefore turbine inlet temperature increases slower .

The air temperature at the compressor exit is calculated by the following equation where the terms $\eta_{is,c}$ and β_c represents compressor efficiency and compressor pressure ratio respectively:

$$T_{out} = T_{in} \times \left[1 + \frac{1}{\eta_{is,c}} \times (\beta_c^{\frac{k-1}{k}} - 1)\right]. \quad (2.5)$$

The temperature at the the turbine exit is calculated by the following equation where the terms $\eta_{is,t}$ and β_t represents turbine efficiency and turbine pressure ratio respectively:

$$T_{out} = T_{in} \times [1 - \eta_t \times (1 - \beta_t^{\frac{k-1}{k}})]. \quad (2.6)$$

As described earlier, a plenum is not added at the exit of turbine because of the assumed choked flow conditions within the turbines.

The compressor mechanical power is calculated through the equation below where the terms g_{in} , P_c and h represent air mass flow rate at inlet of compressor, compressor mechanical power and enthalpy respectively:

$$P_c = g_{in} \times (h_{out} - h_{in}). \quad (2.7)$$

The power produced by expanding gas in turbine is calculated through the equation below where the terms g_{in} , P_t and h represent mass flow rate at inlet of turbine, power produced by expanding gas in turbine and enthalpy respectively:

$$P_t = g_{in} \times (h_{in} - h_{out}). \quad (2.8)$$

Thrust is modeled through the equations given below:

$$\frac{F}{g} = \frac{a_0}{g_c} \times \left(\frac{V_9}{a_0} - M_0 \right). \quad (2.9)$$

$$\frac{V_9}{a_0} = \sqrt{\frac{2}{k-1} \times \frac{\tau_\lambda}{\tau_r \times \tau_c} \times (\tau_r \times \tau_c \times \tau_t - 1)}. \quad (2.10)$$

$$\tau_r = 1 + \frac{k-1}{2} \times M_0^2. \quad (2.11)$$

$$\tau_\lambda = \frac{T_3}{T_0}. \quad (2.12)$$

$$\tau_c = (\pi_c)^{\frac{k-1}{k}}. \quad (2.13)$$

$$\tau_t = 1 - \frac{\tau_r}{\tau_\lambda} \times (\tau_c - 1). \quad (2.14)$$

where F represents thrust, g represents air mass flow rate, g_c is Newton's constant, a_0 is speed of sound, M_0 is inlet Mach number, T_0 is ambient temperature and π_c is compressor pressure ratio.

2.3 Reading The Compressor Map

As a part of the gas turbine simulations, the data provided by the compressor maps of gas turbine engines are digitized and loaded to the simulation code in the form of look-up tables. This procedure is performed following the methodology in [8]. In general, having the speed and pressure ratio values is not enough to read a mass flow rate as there might be two values for mass flow rate at a given pressure ratio. On the other hand, there might be two values for pressure ratio for a given mass flow rate on a rotational speed line that is vertical. The concept of β -lines, as described in [16], are introduced as an additional coordinate system to the compressor map that allows an independent map reading using these lines and rotational speed values. β -lines can be generated as polynomials or straight lines which do not intersect each other and are equally spaced. A general representation of the beta grid generation is given in Figure 2.6.

After β -lines are generated on compressor map, a grid is formed which provides discrete points. The data from those points are used in order to prepare the look up tables. Two look up tables are formed: The first one allows the code to read pressure ratio value knowing the β -line index and the rotational speed value. The second one allows to read mass flow rate value again knowing the β -line index and the rotational speed. The representation of those look up tables are given in Figure 2.7. The efficiency is assumed to be constant in both simulation studies and a third look-up table is not used for efficiency calculations. This feature may be added as a future study.

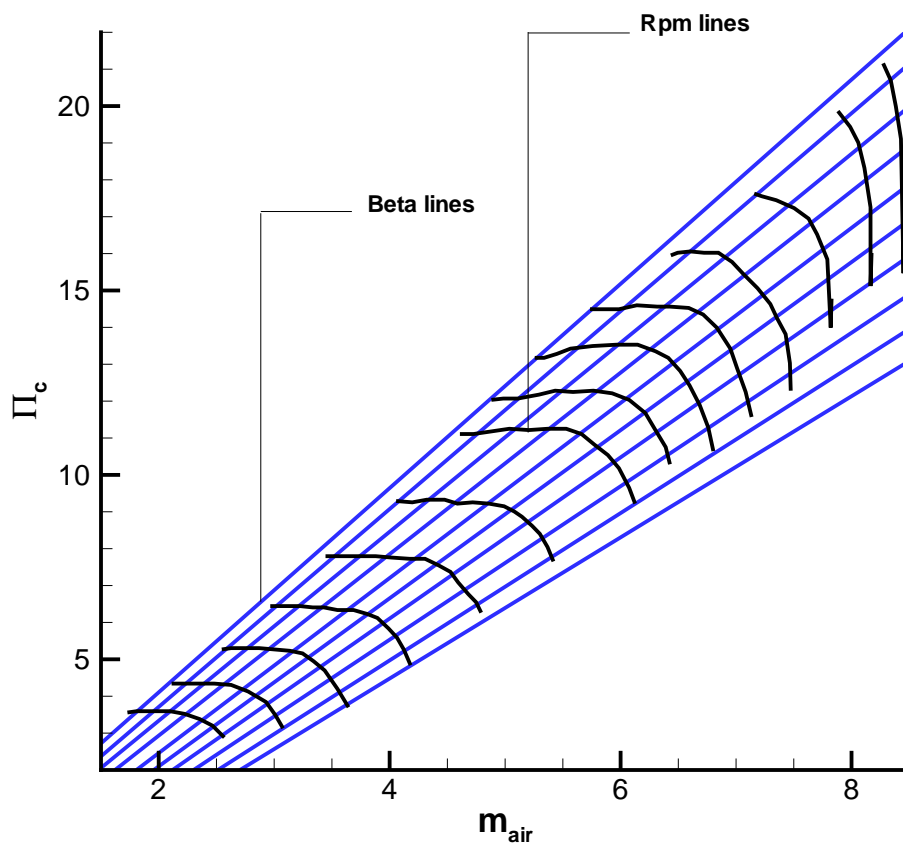


Figure 2.6: Representation of beta lines grid generation.

	Beta1	Beta2	Beta3	Beta4	Beta5	Beta6	Beta7
N1							
N2		↓	→				
N3			pressure ratio				
N4							
N5							
N6							
N7							
N8							
N9							
N10							

	Beta1	Beta2	Beta3	Beta4	Beta5	Beta6	Beta7
N1							
N2		↓	→				
N3			mass flow rate				
N4							
N5							
N6							
N7							
N8							
N9							
N10							

Figure 2.7: Look-up tables data structure produced using the digitized compressor map.

CHAPTER 3

SINGLE SPOOL TURBOJET SIMULATIONS

3.1 Turbojet Engine Characteristics

The aero-thermal transient performance model is first used for the simulation of a small turbojet engine by applying different fuel scheduling scenarios. The response of the turbojet engine model is investigated by monitoring the engine rotational speed, turbine inlet temperature and the thrust level variations.

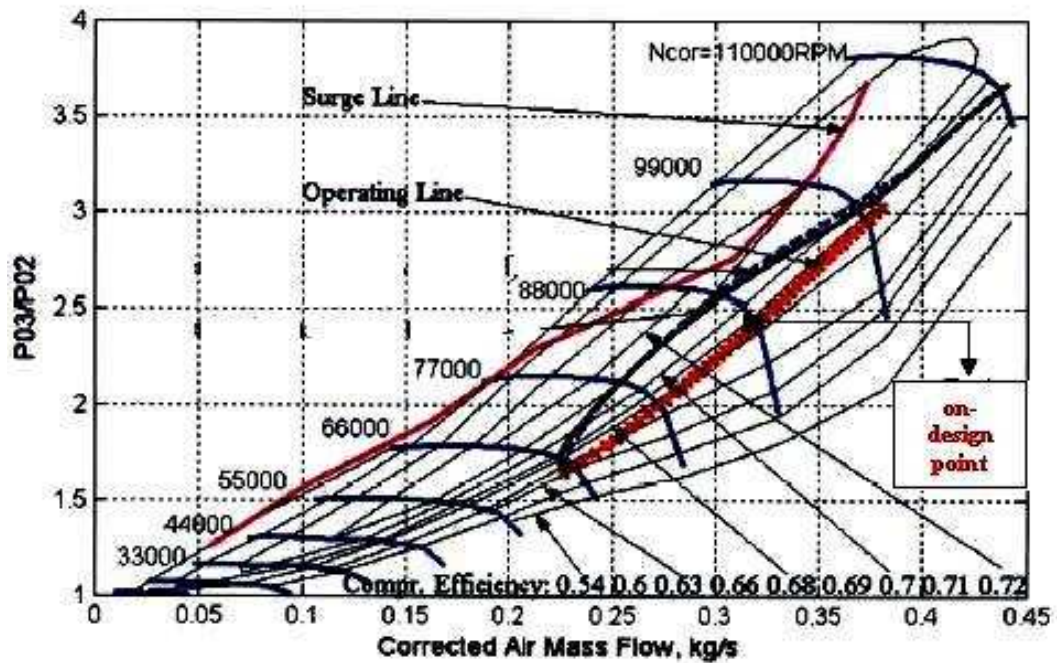


Figure 3.1: A typical compressor map for a small turbojet engine as given in [5].

The design point of the small turbojet engine that is simulated is chosen to be at 30000 ft and at Mach 0.8. The compressor pressure ratio, turbine inlet temperature and the mass flow rate are chosen as 2.45, 1300 K and 0.32 kg/s, respectively, which are typical values for a small turbojet engine with no bleed and no turbine cooling.

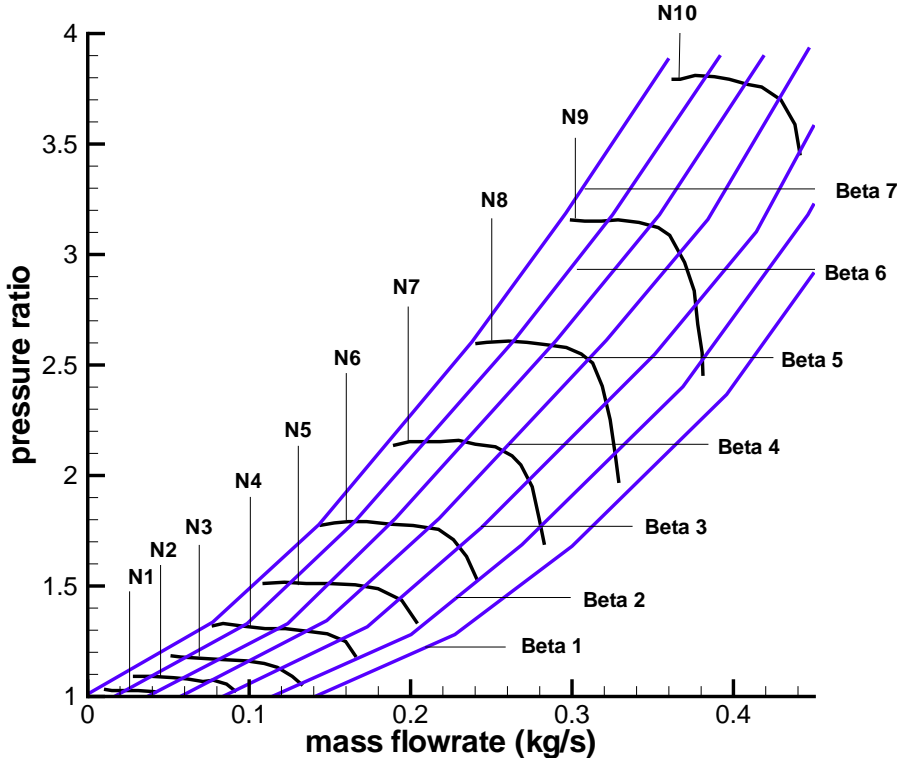


Figure 3.2: The digitized version of the compressor map given in Figure 3.1, which is used to generate the look-up tables.

The compressor map given in [8] is used (Figure 3.1) which has performance characteristics consistent with the simulated turbojet engine. A point on the operating line is marked on that map as the on-design point of the turbojet engine. An on-design cycle analysis is performed following the methodology presented in [15], and outputs are used as the turbojet reference point data and as inputs to the simulation code. The design point thrust level of the engine is 150 N.

The compressor map for the small turbojet engine given in [5] is digitized by using the β -line technique. The original compressor map is given in Figure 3.1 and the digitized version is given in Figure 3.2.

3.2 Results

The response of the small turbojet engine is presented for two sample fuel scenarios that simulates different fuel scheduling applications.

Figure 3.3, Figure 3.4 and Figure 3.5 show the results of the first sample simulation obtained using the code developed as a part of this study. The sample representative scenario consists of five different legs:

- 1) the engine is working at its reference conditions between $t=0$ s and $t=60$ s,
- 2) a step input of about 42% increase in fuel flow rate is applied to the fuel mass flow rate that lasts for another 60 s,
- 3) the fuel flow rate returns back to the reference condition at $t=120$ s,
- 4) another step input is applied at $t=180$ s and
- 5) after an additional 60 s fuel flow rate value returns back to its original reference value and keeps at that level until $t=300$ s.

In Figure 3.3, Figure 3.4 and Figure 3.5, the variations in the engine rotational speed, turbine inlet temperature and engine thrust with the fuel scheduling are presented respectively. All values are normalized against their original levels before the fuel scheduling starts.

During the first 60s, as the fuel flow rate stays at its reference level, all three parameters that are presented also stay at their corresponding reference levels. When a 40% step input is applied to the fuel flow rate, the rotational speed value increases linearly and reaches to a value 6% higher than its reference value at about $t=120$ s. Then it starts to decrease linearly and reaches to its reference value at $t=140$ s. The turbine inlet temperature behaviour follows the

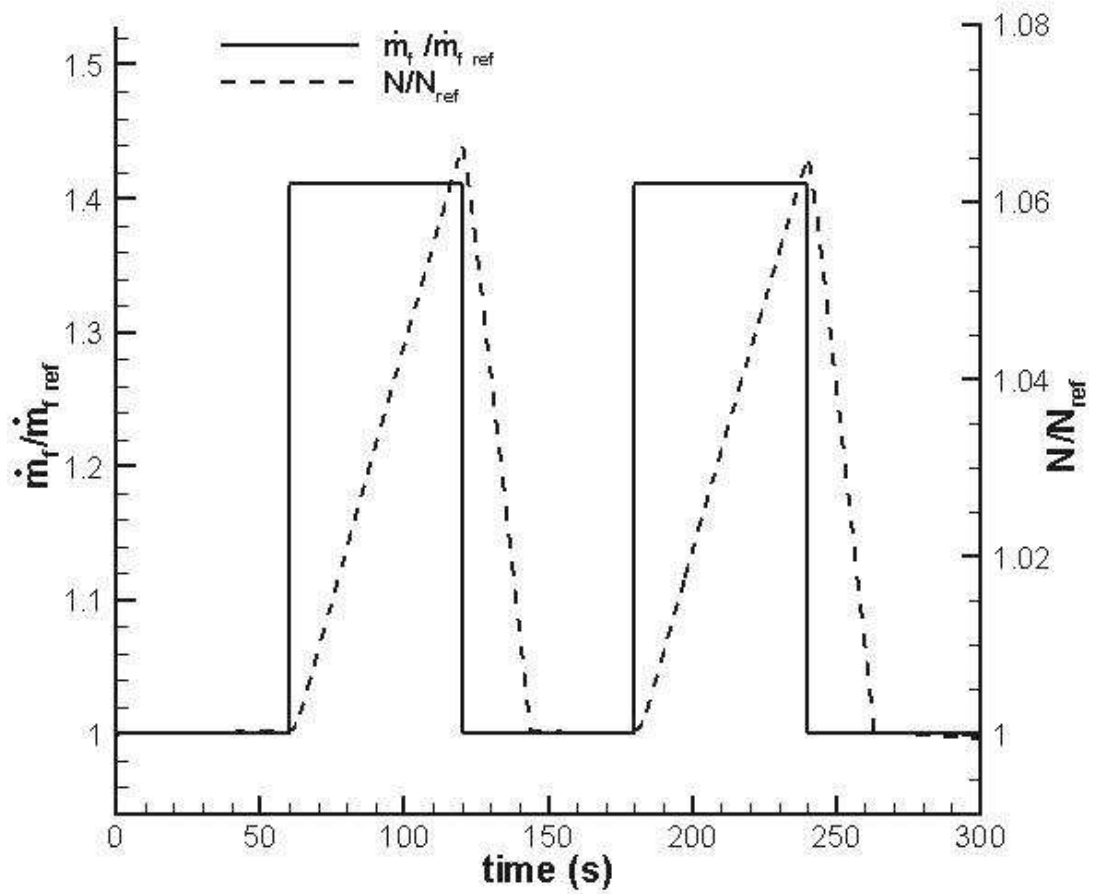


Figure 3.3: The response of small turbojet engine rotational speed to step inputs in the fuel mass flow rate. Turbojet engine simulation scenario 1.

fuel scheduling very closely except for a slight lag in the beginning of the step input (Figure 3.4). As soon as the fuel flow rate is increased 40%, the turbine inlet temperature jumps to a value that is 60% higher than its reference value.

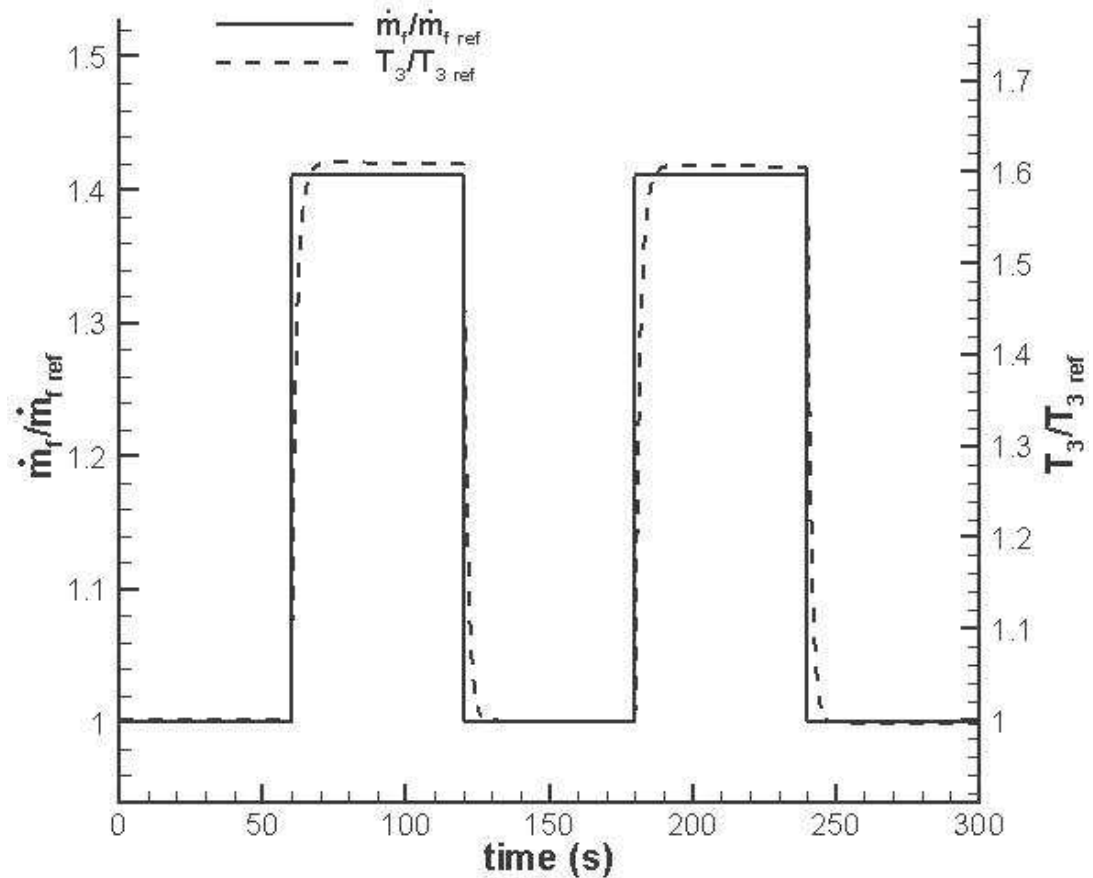


Figure 3.4: The response of small turbojet engine turbine inlet temperature to step inputs in the fuel mass flow rate. Turbojet engine simulation scenario 1.

Figure 3.5 shows that the thrust level also follows the fuel scheduling inputs quite closely, however there exists a slight undershoot followed by an overshoot when the fuel flow rate is suddenly decrease back to its reference level. The thrust value increases to a value 14% higher than its reference value when the step fuel input is applied. As can be seen in Figure 3.3 and Figure 3.5, the lag of thrust response is much smaller than rotational speed response which is found out to be due to the modeling of shaft dynamics. As a future work, shaft

dynamics may be remodeled by using Euler Turbine Equation.

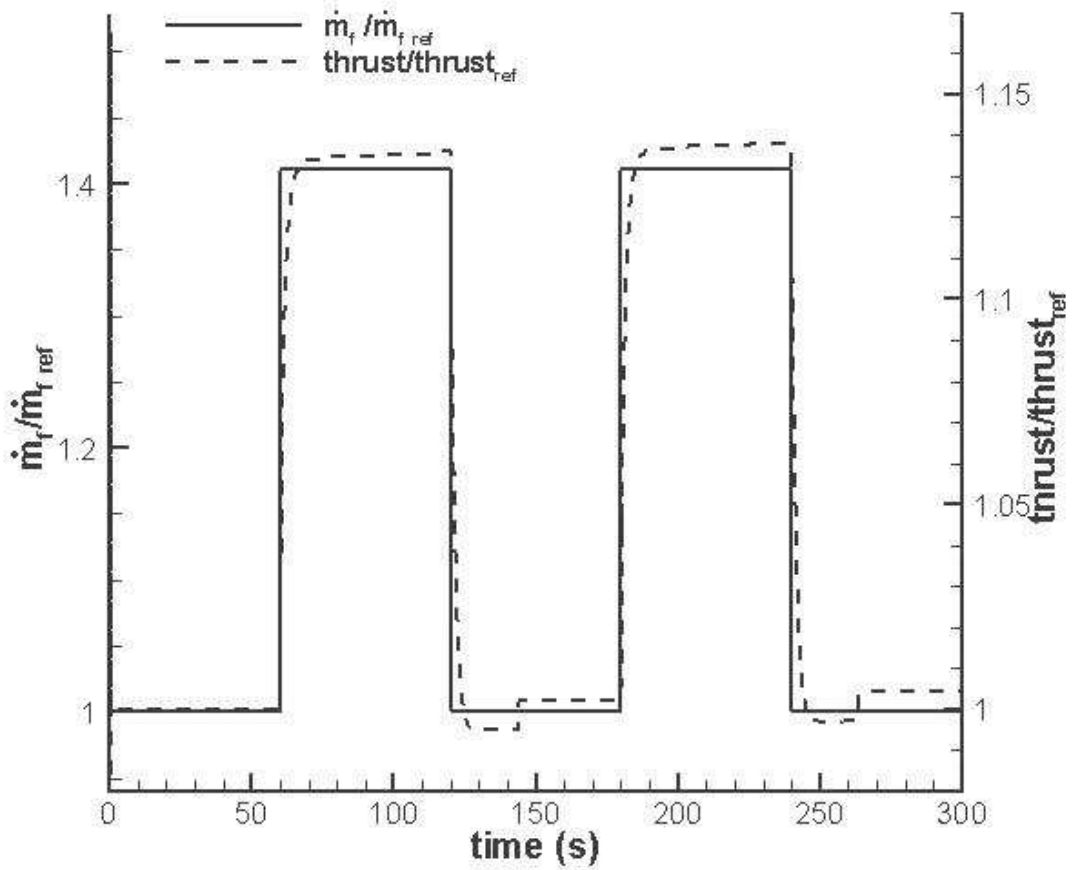


Figure 3.5: The response of small turbojet engine thrust to step inputs in the fuel mass flow rate. Turbojet engine simulation scenario 1.

Figure 3.6, Figure 3.7 and Figure 3.8 show the results of the second sample simulation. This scenario also consists of 5 legs:

- 1) the engine is working at its reference conditions between $t=0$ s and $t=60$ s,
- 2) a linear increase is applied to the fuel mass flow rate that lasts for 60 s till a value of 38% higher than the one at reference point is reached,
- 3) the fuel flow stays at that value for another 60 s,
- 4) returns back to its reference value by decreasing linearly at $t=240$ s and

5) stays at that value till $t=300$ s.

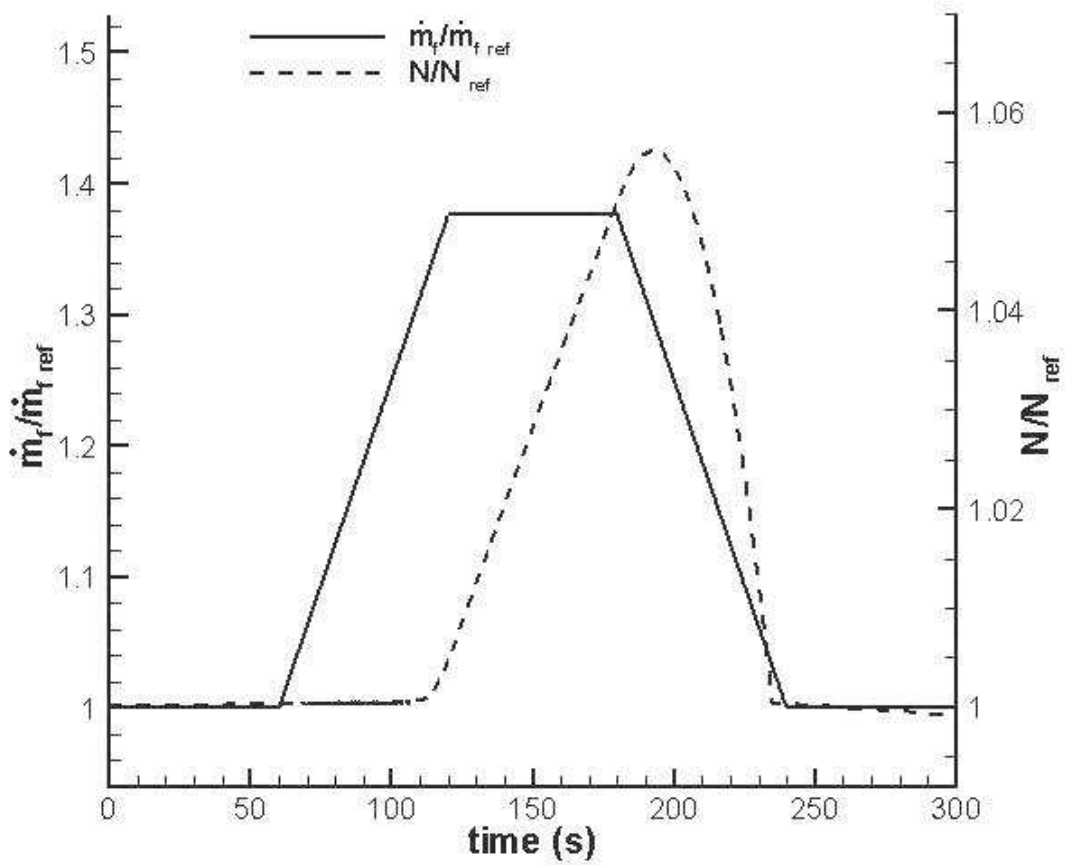


Figure 3.6: The response of small turbojet engine rotational speed to linear increase and decrease in the fuel mass flow rate. Turbojet engine simulation scenario 2.

The rotational speed responds to fuel flow rate increase after about a 50 s delay due mainly to the J term in equation 2.1 which is the moment of inertia of the jet engine. Then rotational speed increases linearly to a value which is nearly 6% higher than its reference value. As the fuel flow rate starts to decrease, after a few seconds, rotational speed value starts to decrease and reaches to its reference value at $t=240$ s and stays at that level until $t=300$ s.

Similar to the previous scenario, the turbine inlet temperature and the thrust variations follow closely the variations in the fuel flow rate.

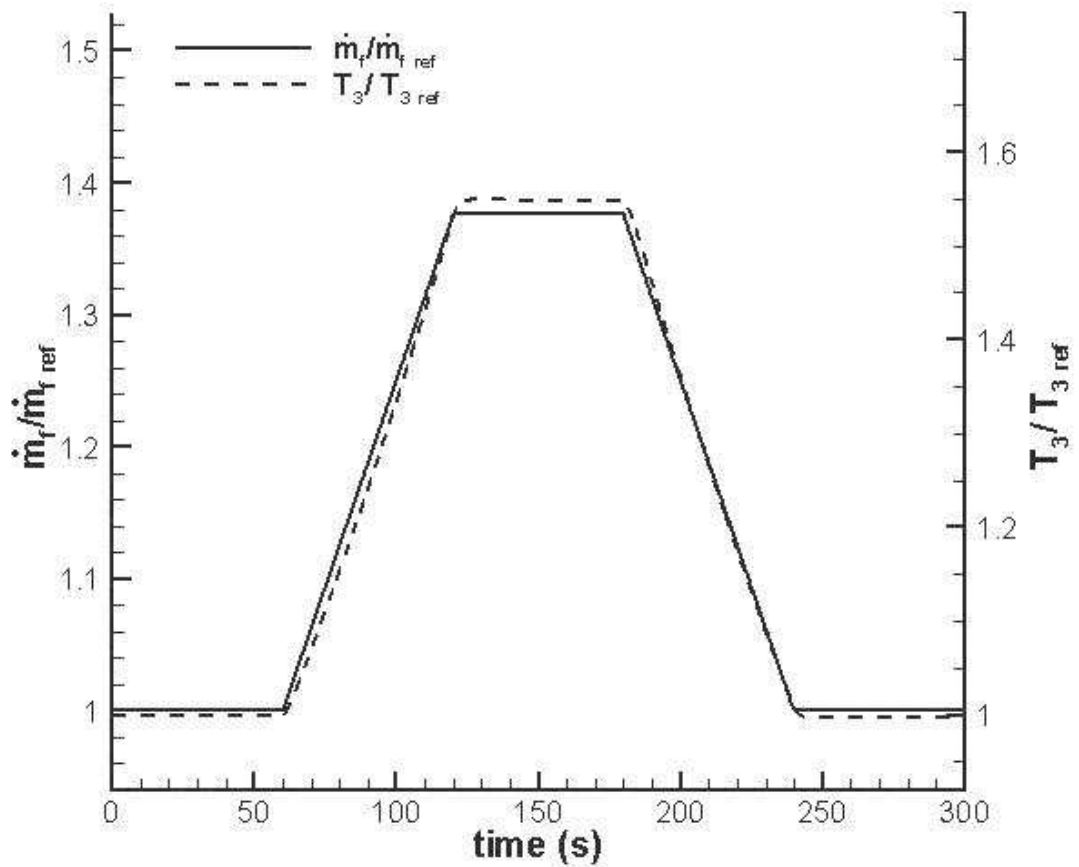


Figure 3.7: The response of small turbojet engine turbine inlet temperature to linear increase and decrease in the fuel mass flow rate. Turbojet engine simulation scenario 2.

The turbine inlet temperature reaches to a value which is 55% higher than its reference value. This rise is slightly smaller than the previous scenario, which had a 60% rise in the temperature, most probably due to the relatively slow increase in the fuel flow rate.

The thrust level also increases about slightly less than 13%, which is again smaller than the 14% increase in the previous scenario.

As a second part of the small turbojet simulation study, lag characteristics of the engine rotational speed is investigated. As a result of the investigation, the engine inertia value is found out to be larger than the value which belongs to

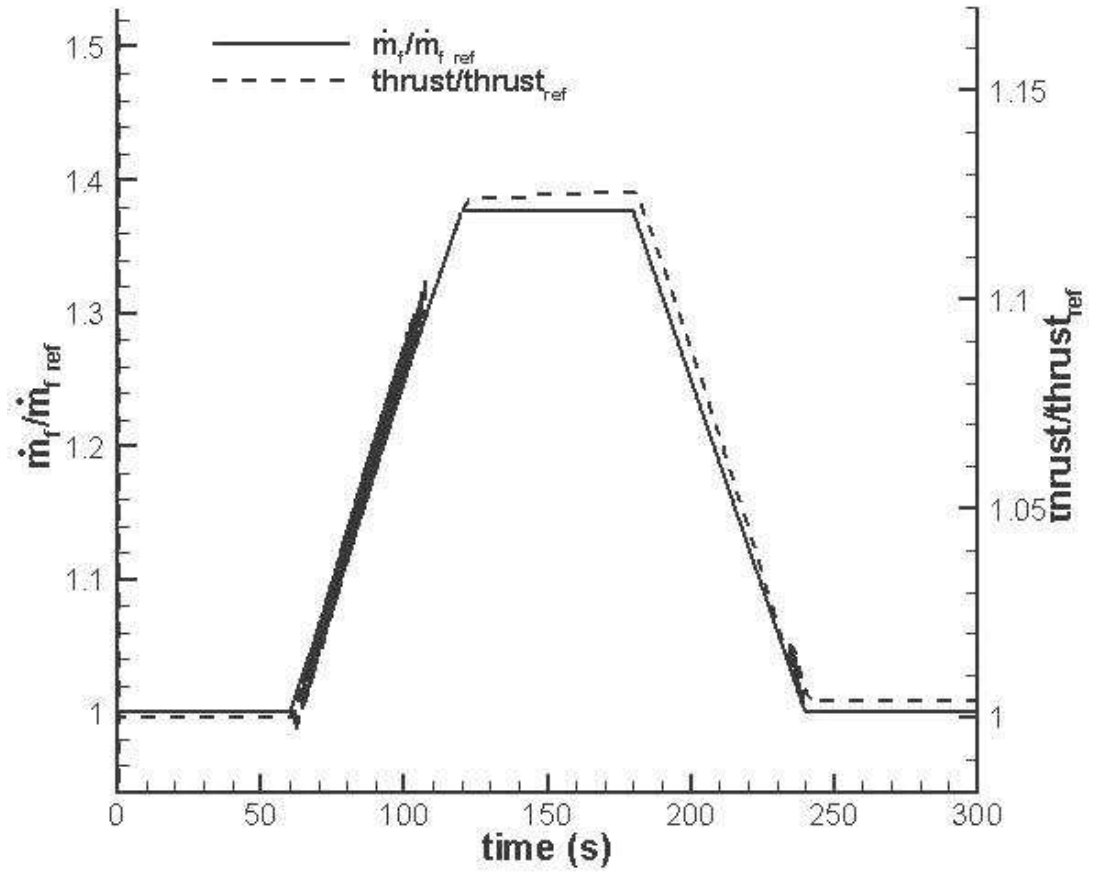


Figure 3.8: The response of small turbojet engine thrust to linear increase and decrease in the fuel mass flow rate. Turbojet engine simulation scenario 2.

a small turbojet engine having the same dimensions as the one in the simulation study and recalculated. The first inertia value that causes the lag of the rotational speed response was calculated using the inertia calculation tool called FESTO [18] by inputting dimensions of the shaft and other rotating components. Same tool is used to calculate several moment of inertia terms and these terms are used as inputs to the simulation code for the first fuel scheduling scenario. As a result of this study, moment of inertia versus lag time curve is plotted which is given in Figure 3.9. Lag time is the time that it takes the engine to reach the next steady state condition in terms of the rotational speed. A moment of inertia term smaller than the one used in previous simulation is input to the turbojet simulation code and the study is repeated with this new inertia value.

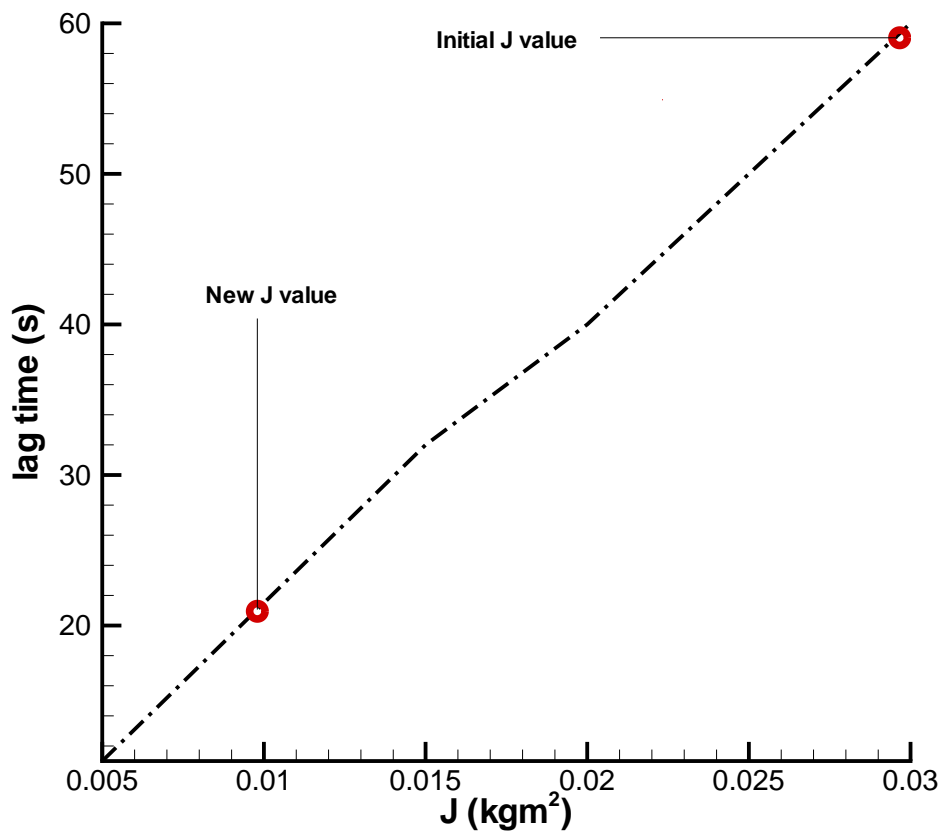


Figure 3.9: Engine moment of inertia term versus lag of engine rotational speed in time.

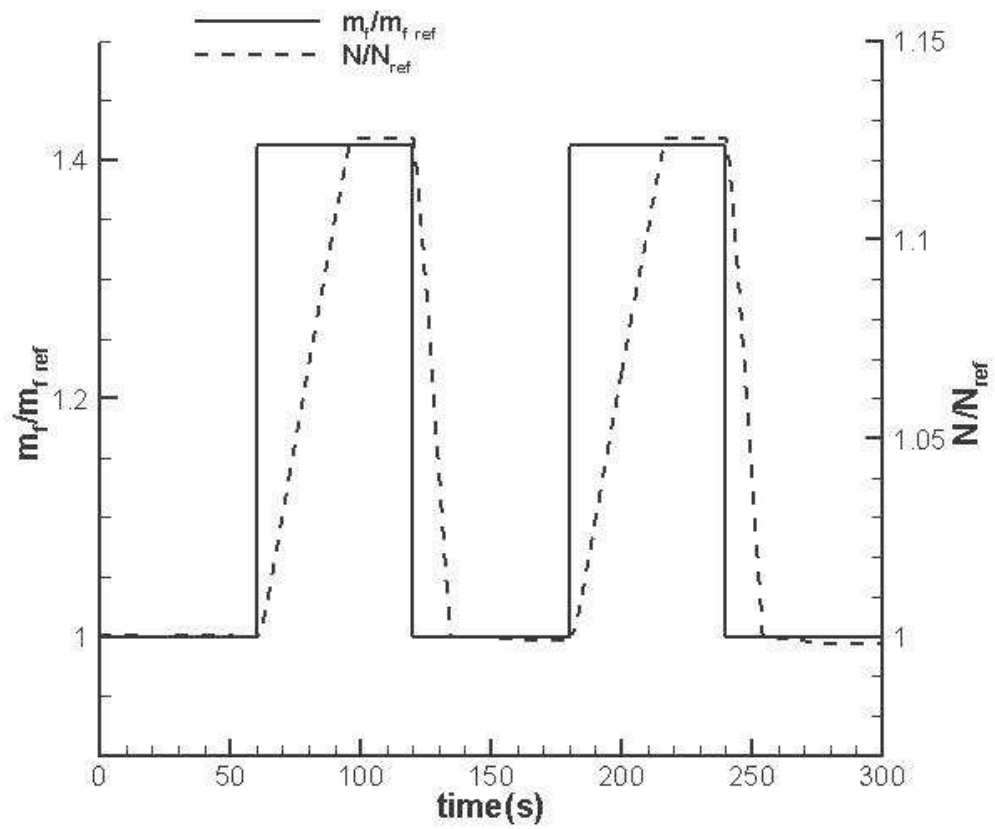


Figure 3.10: The response of small turbojet engine rotational speed to step inputs in the fuel mass flow rate. Turbojet engine simulation scenario 1 with the new engine inertia term.

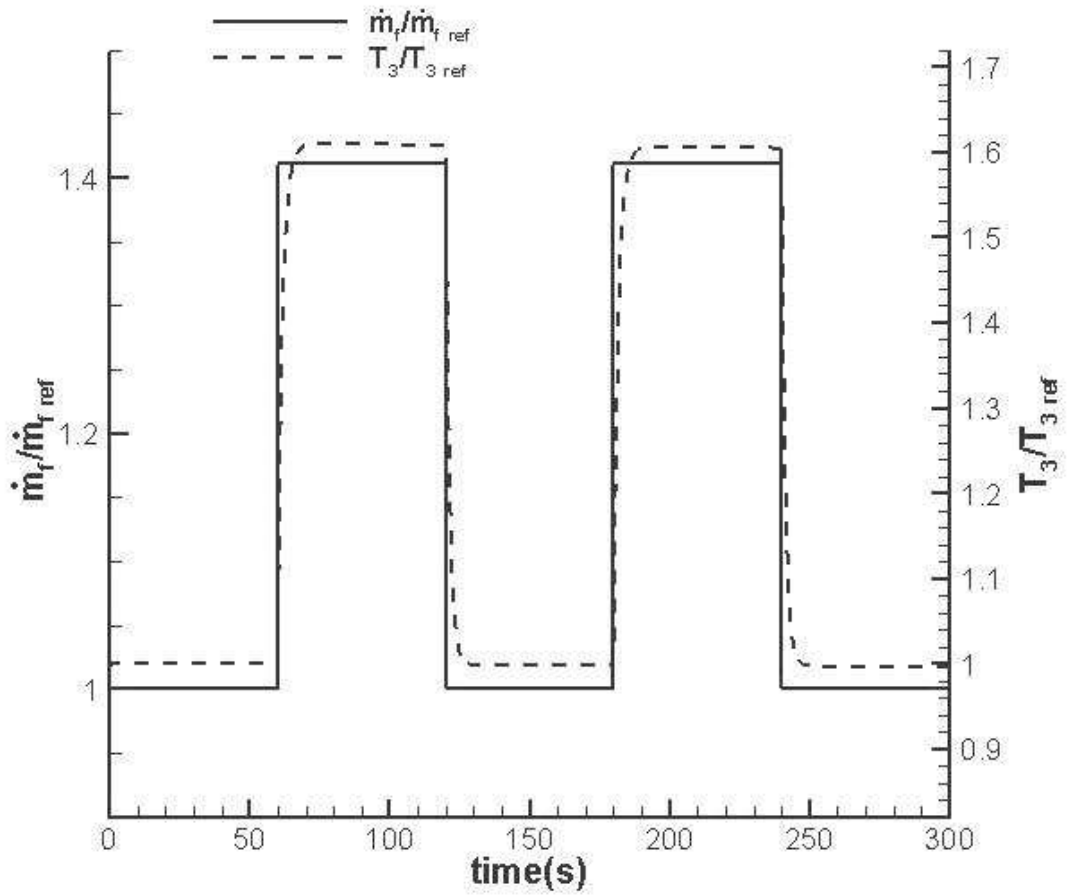


Figure 3.11: The response of small turbojet engine turbine inlet temperature to step inputs in the fuel mass flow rate. Turbojet engine simulation scenario 1 with the new engine inertia term.

In Figure 3.10, 3.11, 3.12, the plots of response of engine rotational speed, turbine inlet temperature and thrust, respectively, to first fuel scheduling scenario with new engine inertia value are presented.

As shown in Figure 3.10, engine rotational speed value follows the fuel flow rate input with less lag in time to reach a constant value when the fuel flow rate is constant at leg 2 and 4 compared with the first simulation result. Different from the first simulation result, inharmonious behaviour of the engine rotational speed with respect to the fuel flow input is diminished in the second simulation case.

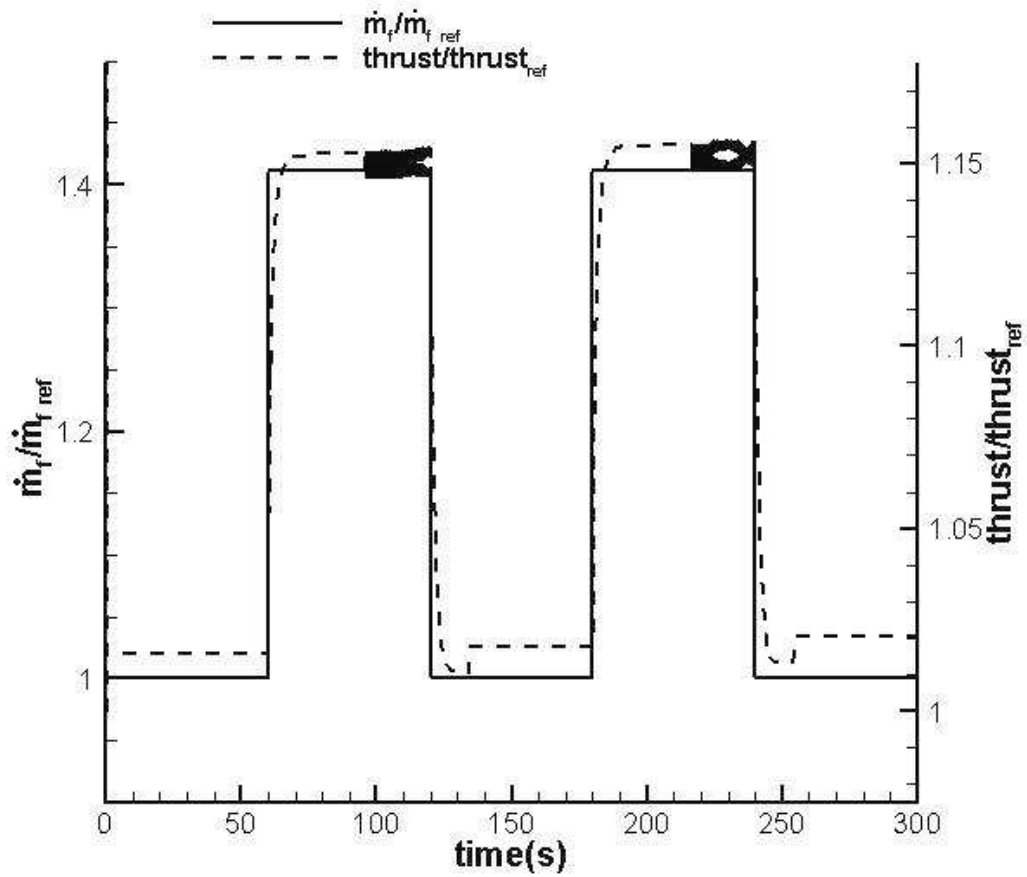


Figure 3.12: The response of small turbojet engine thrust to step inputs in the fuel mass flow rate. Turbojet engine simulation scenario 1 with the new engine inertia term.

As shown in Figure 3.11, turbine inlet temperature follows the fuel flow rate input which is the same response as before. The new J value directly affects the engine rotational speed because of the dominant characteristics of J term in shaft dynamics equation. The change in rotational speed directly affects the air mass flow rate which has a secondary effect on thrust calculations. On the other hand, in turbine inlet temperature modeling equation there is no dominant term related to J directly. There are turbine inlet and outlet mass flow rate terms in the equation but they do not have a sound effect in the result of the equation. Therefore there is no change induced by the the change in J term in turbine inlet temperature calculation results.

Thrust response of the engine with less inertia which is given in Figure 3.12 is same as the one with larger inertia except some oscillations introduced at leg 2 and 4. These oscillation occurs during the period when the rotational speed is constant, and mainly introduced due to the compressor map reading technique which consists of look up tables. As an improvement to compressor map reading technique, these look up tables may be replaced with a neural network-based algorithm which defines continuous functions. These oscillations are expected to be damped out with a neural network based approach, which may be performed as a future study.

In Figure 3.13, Figure 3.14 and Figure 3.15, the plots of response of engine rotational speed, turbine inlet temperature and thrust to second fuel scheduling scenario with new engine inertia value and slight difference in second fuel flow rate scenario are presented. The fuel flow rate increment value per time step is increased in order to provide a faster response of engine parameters to the fuel flow rate scenario.

As shown in Figure 3.13, engine rotational speed responds with a less lag in time and instead of inharmonious behaviour with respect to the fuel flow rate input, it reaches to a constant value at the end of leg 2 when the fuel flow rate input is constant.

It can be seen in Figure 3.14 that turbine inlet temperature follows the fuel flow

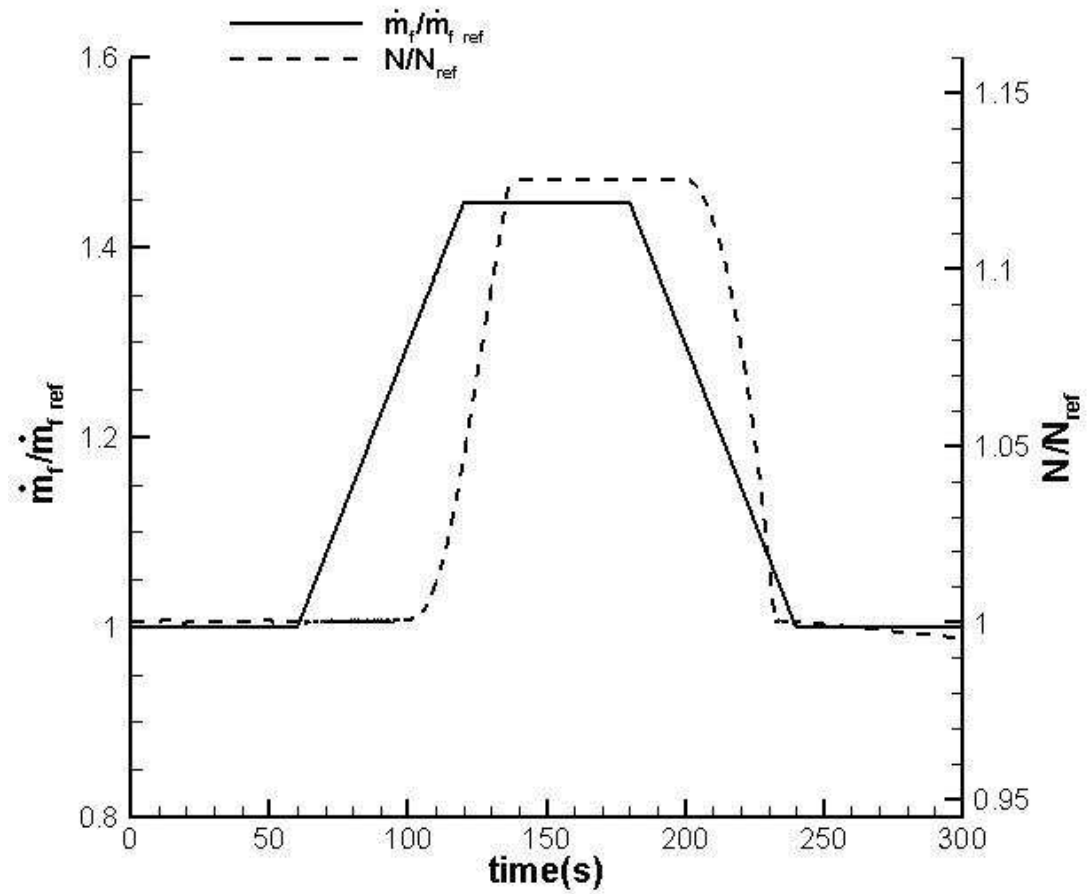


Figure 3.13: The response of small turbojet engine rotational speed to linear increase and decrease in the fuel mass flow rate. Turbojet engine simulation scenario 2 with the new engine inertia term.

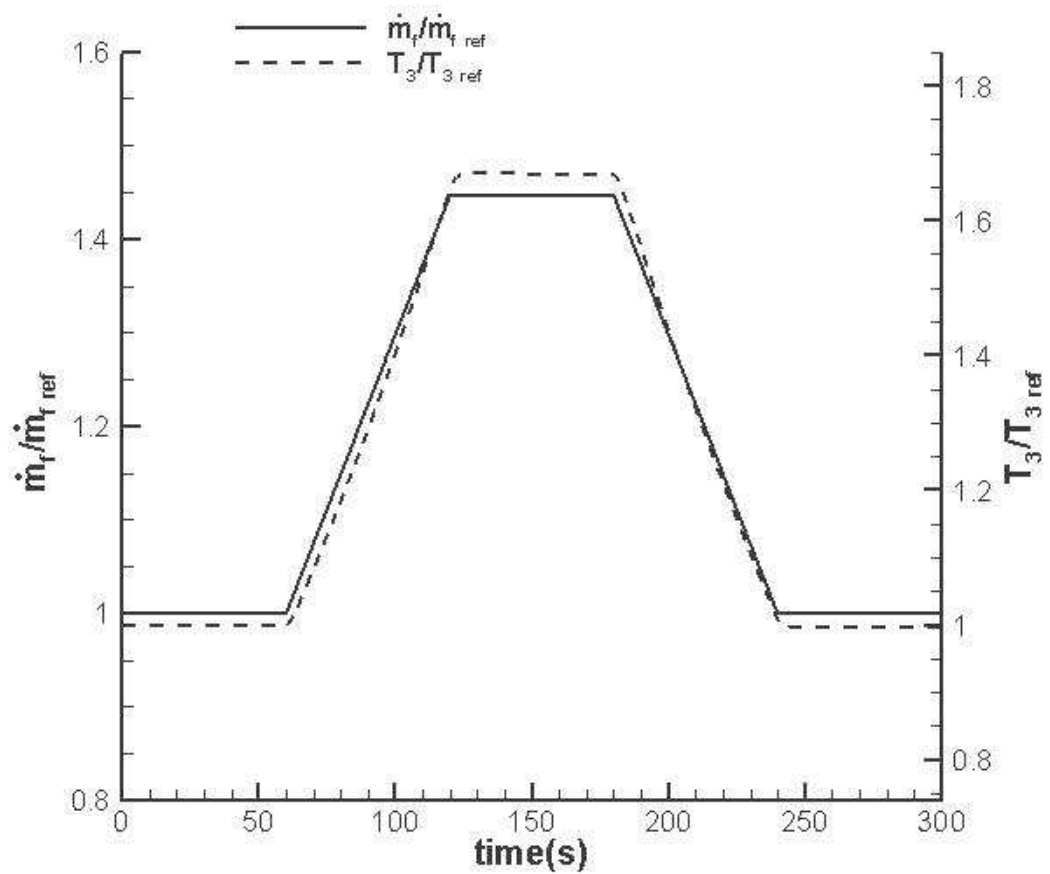


Figure 3.14: The response of small turbojet engine turbine inlet temperature to linear increase and decrease in the fuel mass flow rate. Turbojet engine simulation scenario 2 with the new engine inertia term.

rate input which is the same response in the first simulation case with larger inertia value and less fuel flow rate increment.

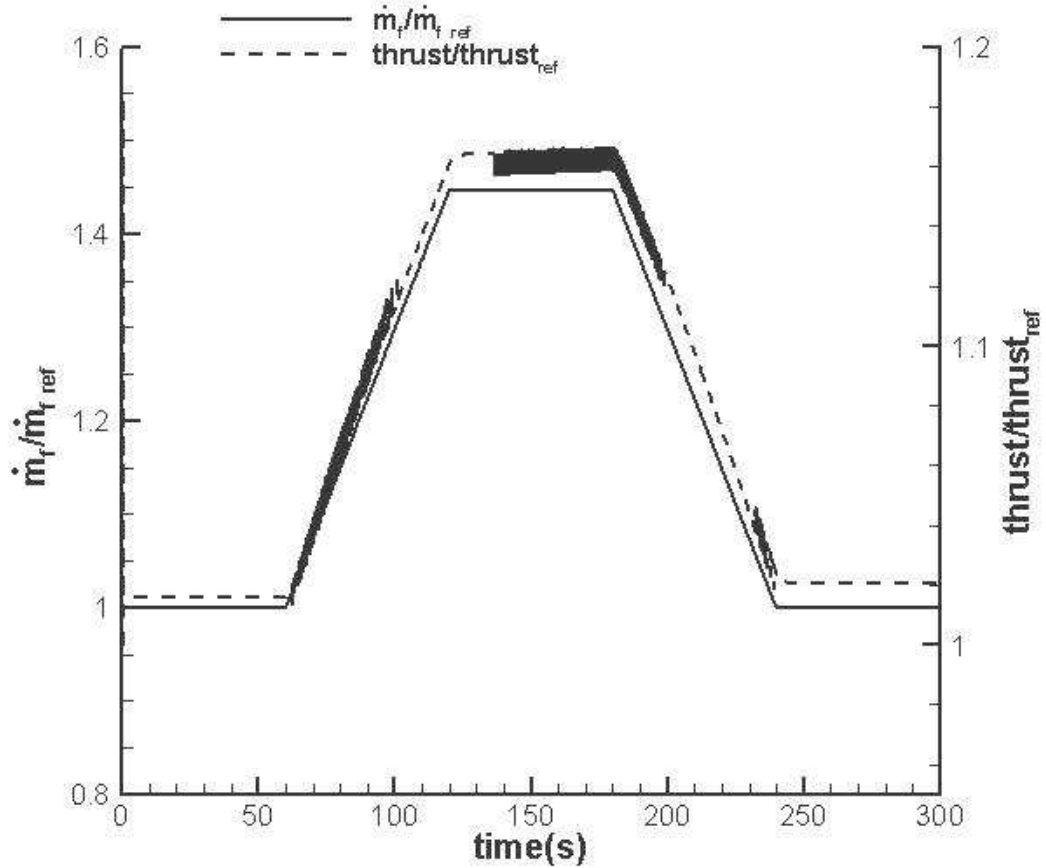


Figure 3.15: The response of small turbojet engine thrust to linear increase and decrease in the fuel mass flow rate. Turbojet engine simulation scenario 2 with the new engine inertia term.

Figure 3.15 shows that thrust response is also the same as the first simulation case except the new oscillations introduced at leg 2 and 3. These oscillations which exists at both first and second ramp fuel input simulation cases are found out to be due to the look up table representation of the compressor map. These oscillations are expected to be damped out with a fine β -line grid used in compressor map reading technique.

The conclusion of the study performed to investigate the lag characteristic of the engine rotational speed is summarized as follows: The response of rotational

speed is improved and lag becomes slightly smaller and inharmonious behaviour with respect to the fuel flow rate input is diminished by using a smaller inertia value as input and increasing the fuel input increment value at the second simulation case. However there still exists a lag of rotational speed comparing with thrust. The mathematical background of this lag is also investigated through the equation of shaft dynamics modeling. It is found out that until the fuel flow rate increases to a certain value, the difference of compressor and turbine power term remains nearly constant which means the change in compressor and turbine power terms cancel each other and as a result no change in engine model rotational speed response is observed in this period. This issue is turned out to be a shaft dynamics modeling problem. As a future work, shaft dynamics may be re-modelled by taking the turbomachinery concept into consideration by using the Euler turbomachinery equation.

CHAPTER 4

COMPARISON OF SINGLE SPOOL TURBOJET ENGINE SIMULATIONS WITH TEST DATA

In order to validate the performance of the generic gas turbine engine simulation code, an experimental study for a small turbojet engine is performed by measuring the transient response of a small turbojet engine to variations in the fuel flow rate. The fuel flow rate input which corresponds to the rotational speed scenario is recorded. Engine rotational speed, engine thrust and exhaust gas temperature values are measured and the results are plotted. The fuel flow rate scheduling used in the tests are input to the simulation code and the responses of thrust and rotational speed response characteristics are compared with the experimental results.

4.1 Experimental Set-up

The SIMJET turbojet engine, of which the specifications are given in Table 4.1 is used in the experiments. SIMJET turbojet engine is a small engine which is 113 mm in diameter and 300 mm in length. It has an idle rotational speed of 28000 rpm and an idle thrust of 0.6lb(2.7N). The maximum thrust delivered by SIMJET is 22lb(100N) and its maximum rotational speed is 120000 rpm. SIMJET turbojet engine has an Engine Control Unit(ECU) which performs the following functions [19]:

- *Automated start-up sequence:* The ECU determines when to apply starter power, glow drive, propane and fuel to the system.

- *Throttle control*: The ECU translates the throttle signal directly to compressor RPM for more linear thrust response characteristics. The throttle signal from the receiver is read using an optocoupler interface to resist EMC noise transmission problems.
- Idle stabilization with indicator (yellow LED)
- Automatic glow plug drive and fault detection circuitry.
- Compressor RPM monitor: Engine speed is continually monitored and is not permitted to exceed the maximum rpm value programmed in the ECU.
- Auto Shut Down (ASD): In case of overspeed, overtemp, or loss of throttle signal the ECU will immediately stop fuel flow to the engine.
- Provides status information to the Cockpit Display Panel.

Table 4.1: Specifications of the SimJet turbojet engine.

Parameter	Value	Unit
<i>MaxThrust</i>	22/100	<i>lbs/N</i>
<i>MaxRotationalSpeed</i>	120000	<i>rpm</i>
<i>IdleRotationalSpeed</i>	28000	<i>rpm</i>
<i>IdleThrust</i>	0.6/2.7	<i>Ibs/N</i>
<i>Pressureratio</i>	2:1	
<i>ExhaustGasTemp@MaxRPM</i>	630	$^{\circ}C$
<i>Fuelconsumption@MaxRPM</i>	259/8,75	<i>mL/oz</i>
<i>Fuel</i>	Jet A1	
<i>Lengthwithstarter</i>	300	<i>mm</i>
<i>Lengthwithoutstarter</i>	220	<i>mm</i>
<i>Diameter</i>	113	<i>mm</i>
<i>Weight</i>	1275	<i>g</i>

The turbojet engine is mounted on free sliding bars which allow the engine to move freely on the thrust axis. A 200 N range miniature load cell is placed in front of the system directly as shown in Figure 4.1. Also in Figure 4.1, FADEC unit, fuel pump and solenoid valves on fuel and propane lines which enables or disables fuel flow through the lines can be seen on the test set-up.

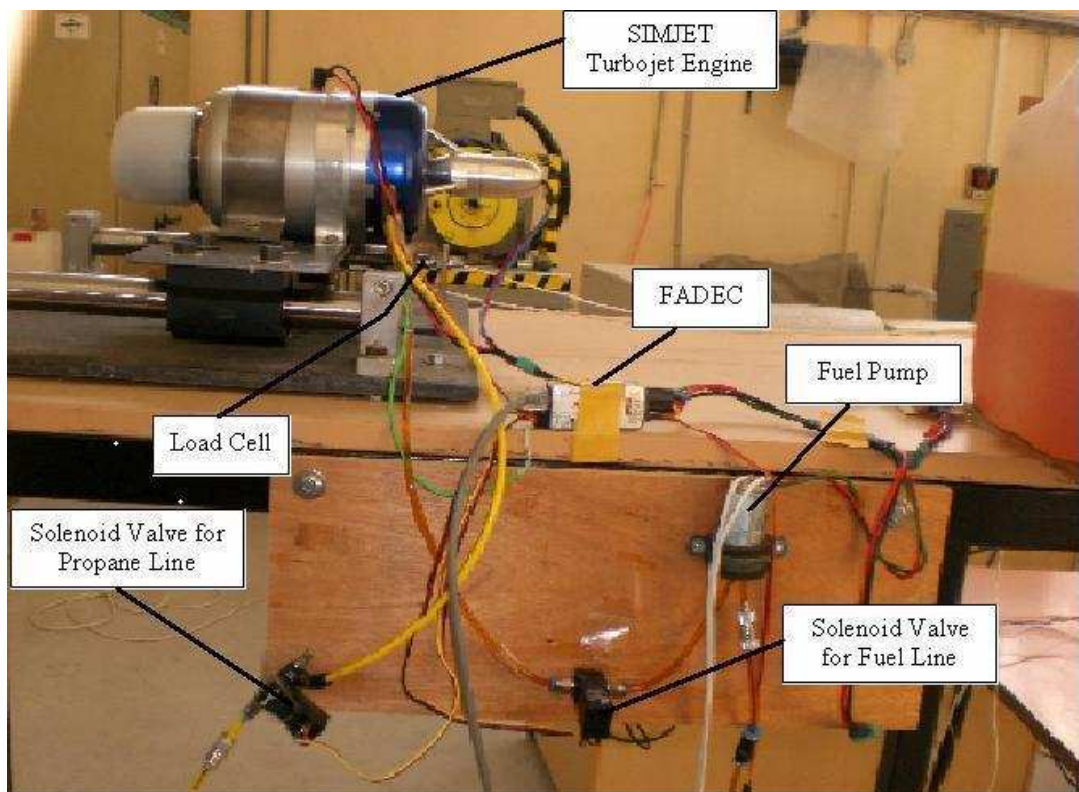


Figure 4.1: Small turbojet engine test setup.

4.2 Experimental Methods

SIMJET engine is first started by the help of an electric motor. As the electric motor is started, propane is pumped through the propane line into the combustion chamber until the temperature inside the chamber reaches to 100°C. Before the engine rotational speed reaches to 30000 rpm which was set as the idle rpm value for the SIMJET, at the time when the temperature reaches to 100°C, liquid fuel is started to be pumped into the combustion chamber. After the engine starts to operate at the idle rpm value, a fuel scheduling scenario is applied through the control panel.

A quasi-step rotational speed input are applied several times subsequently to the small turbojet engine. Variations of thrust, engine rotational speed and exit temperature values are recorded.

The scenario applied during the experiments consists of six legs:

- 1) the engine runs at idle with 30000 rpm and corresponding fuel flow rate is applied until $t=40$ s,
- 2) a quasi-step input of about 50% increase in fuel flow rate is applied to the fuel mass flow rate that lasts for another 45 s which is the fuel flow rate value at 50000 rpm,
- 3) the fuel flow rate returns back to the value at idle at $t=85$ s,
- 4) another quasi-step input is applied at $t=120$ s and after an additional 100s, fuel flow rate value returns back to the value at idle at $t=220$ s,
- 5) then fuel flow rate stays at its value at idle for 15s,
- 6) at $t=235$ s, another quasi-step input of 50% increase in fuel flow rate is applied and keeps at that level until $t=290$ s then for 10 seconds the fuel flow rate stays at its value at idle. When the engine is off, fuel flow rate is decreased to zero at $t=303$ s.

A simple video recorder is used for data acquisition. The video data is converted

to the digital format through a computer software and the frames are separated. The necessary data are collected from the digital displays that are in the field of view of the camera. The data acquisition frequency is kept at 1 Hz which was sufficient to investigate the engine transients.

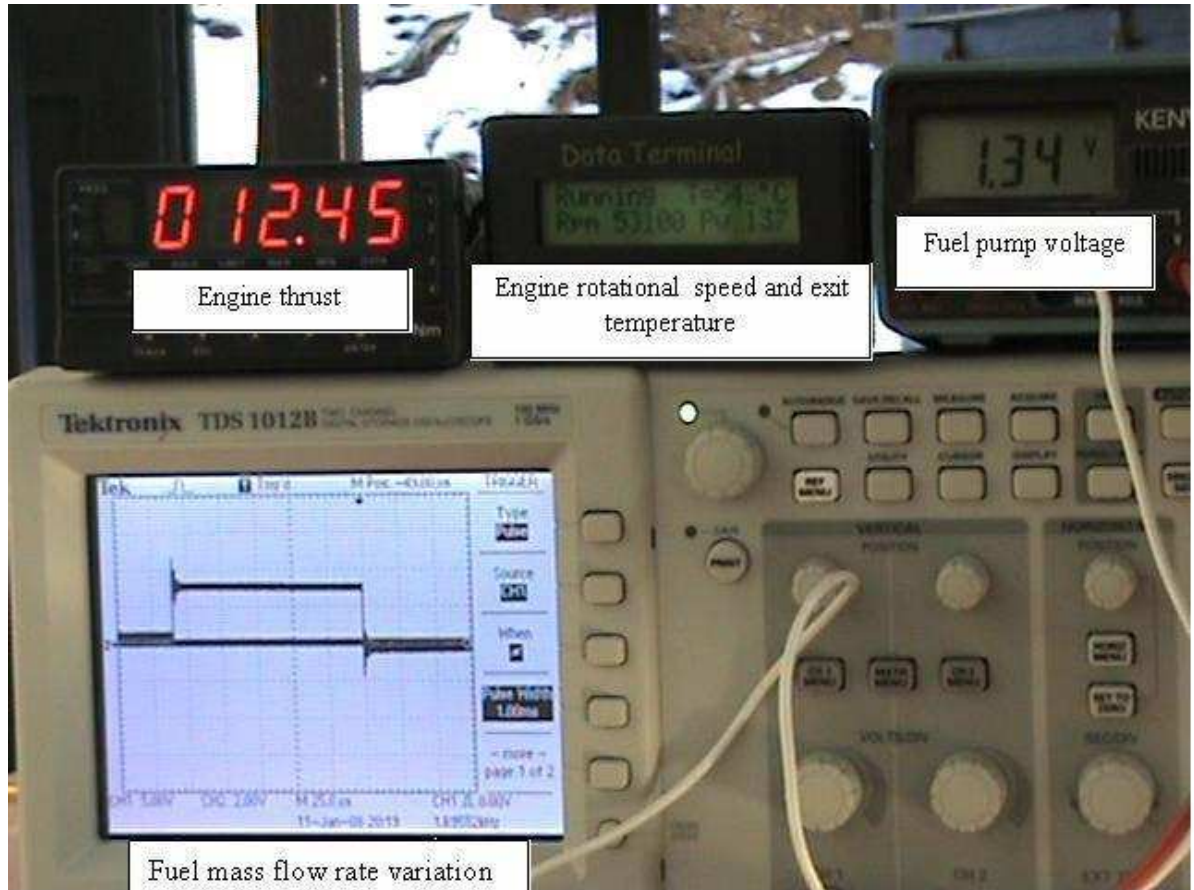


Figure 4.2: Data Acquisition Control Panel used in the turbojet experiments.

As can be seen in Figure 4.2, thrust value that is measured by the load cell is displayed on a load cell display unit. Fuel mass flow rate value is measured through the voltage of the fuel pump. A digital oscilloscope is used for visualizing the fuel scheduling variations. Engine rotational speed and engine exit temperature values are read from the engine controller screen.

The fuel pump voltage values measured by the voltmeter are transformed into fuel flow rate values by using the calibration curve of fuel pump given in Figure 4.3 which was obtained and presented in [21].

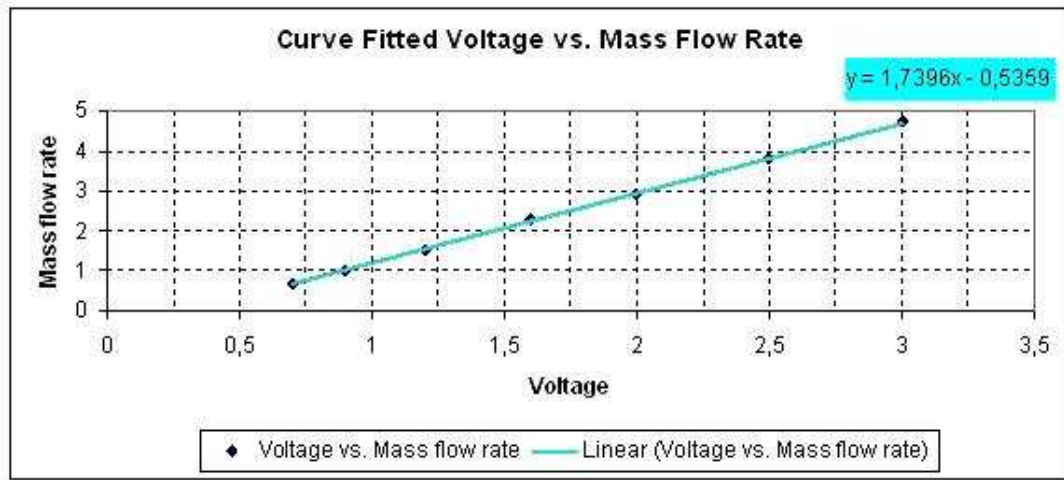


Figure 4.3: Fuel Pump voltage versus fuel mass flow rate curve for the SIMJET Engine [21].

4.3 Experimental Results

Figure 4.4, Figure 4.5 and Figure 4.6 show the responses in the engine rotational speed, engine thrust and exhaust gas temperature, respectively, as the fuel scheduling scenario described previously is applied. At all legs of the scenario engine rotational speed and engine thrust follows the fuel flow rate behavior very closely. Behaviors of engine rotational speed and engine thrust are almost the same as the fuel flow rate.

As it can be seen at Figure 4.6, engine exhaust gas temperature varies within a small range showing a nearly constant behavior with a small difference between two legs when the engine runs at idle and at 50000rpm. When the engine is commanded to run at 50000 rpm, a sudden increase at engine exit temperature is observed due to the increase in fuel flow rate and then the temperature value reaches to a value which is nearly the same as the value at 30000 rpm. This behaviour can be explained by the action of the ECU which is a part of SimJet engine test facility. The ECU directly controls the fuel pump and adjusts the fuel flowrate value by using the exhaust gas temperature as feedback. This control algorithm tries to keep the exhaust gas temperature value in a margin in order to avoid an overspeed or possible engine damage.

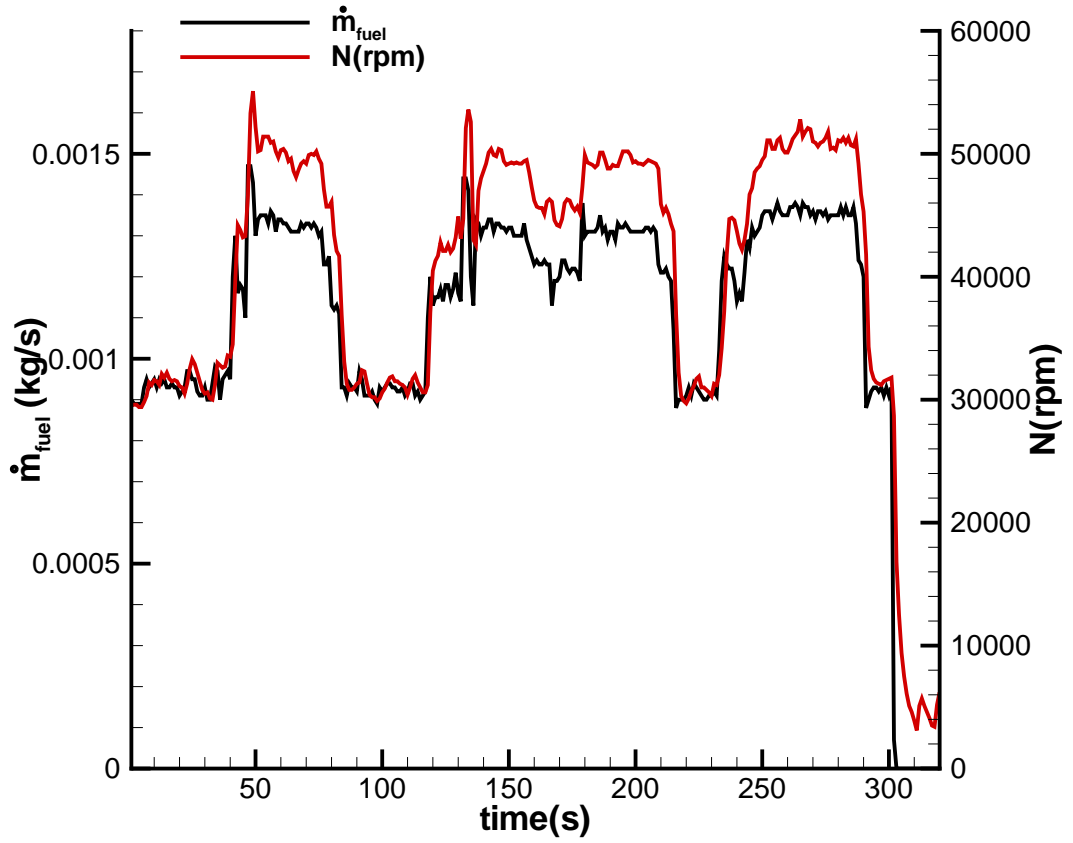


Figure 4.4: The response of engine rotational speed to quasi-step inputs in the fuel mass flow rate.

4.4 Comparison of the Experimental Results with Simulation Results

In order to investigate the response of the turbojet engine model to the fuel flow rate scenario applied in the experiments, same fuel flow variations are applied to the simulation code and engine rotational speed, thrust and exhaust gas temperature responses are compared with the results of the experiment. The purpose of this study was not to perform a direct numeric comparison of the model response with the experimental results. In this study, trends of the

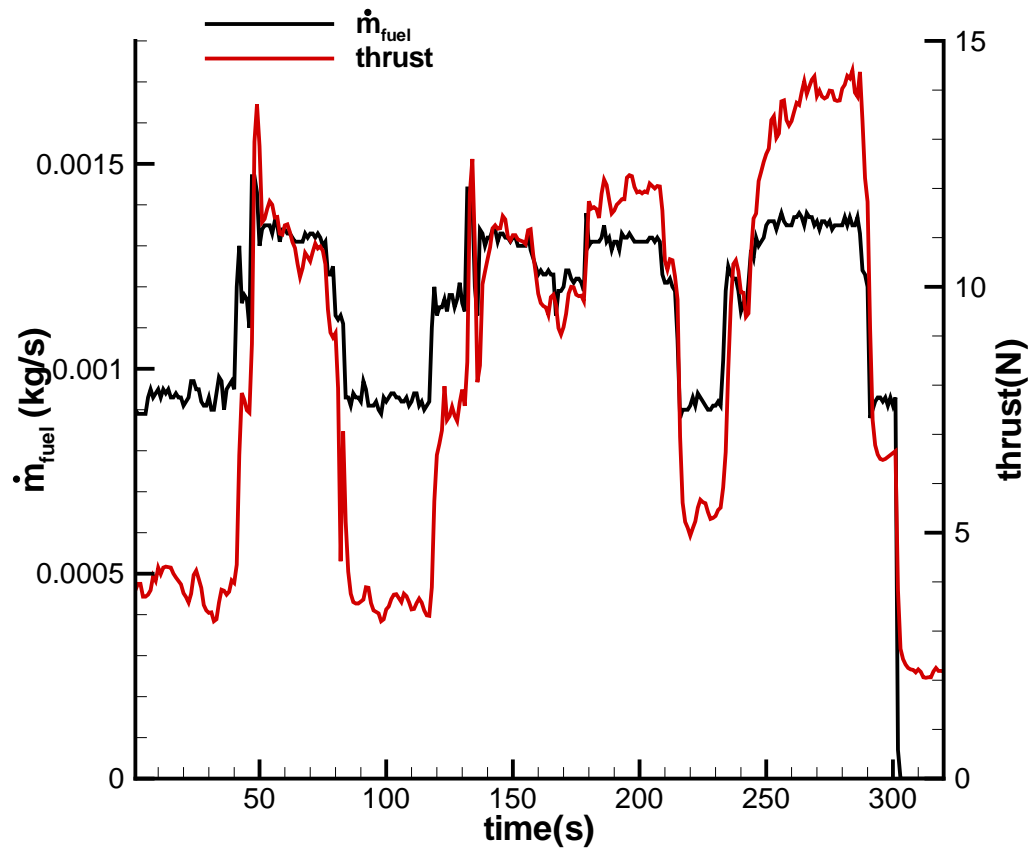


Figure 4.5: The response of engine thrust to quasi-step inputs in the fuel mass flow rate.

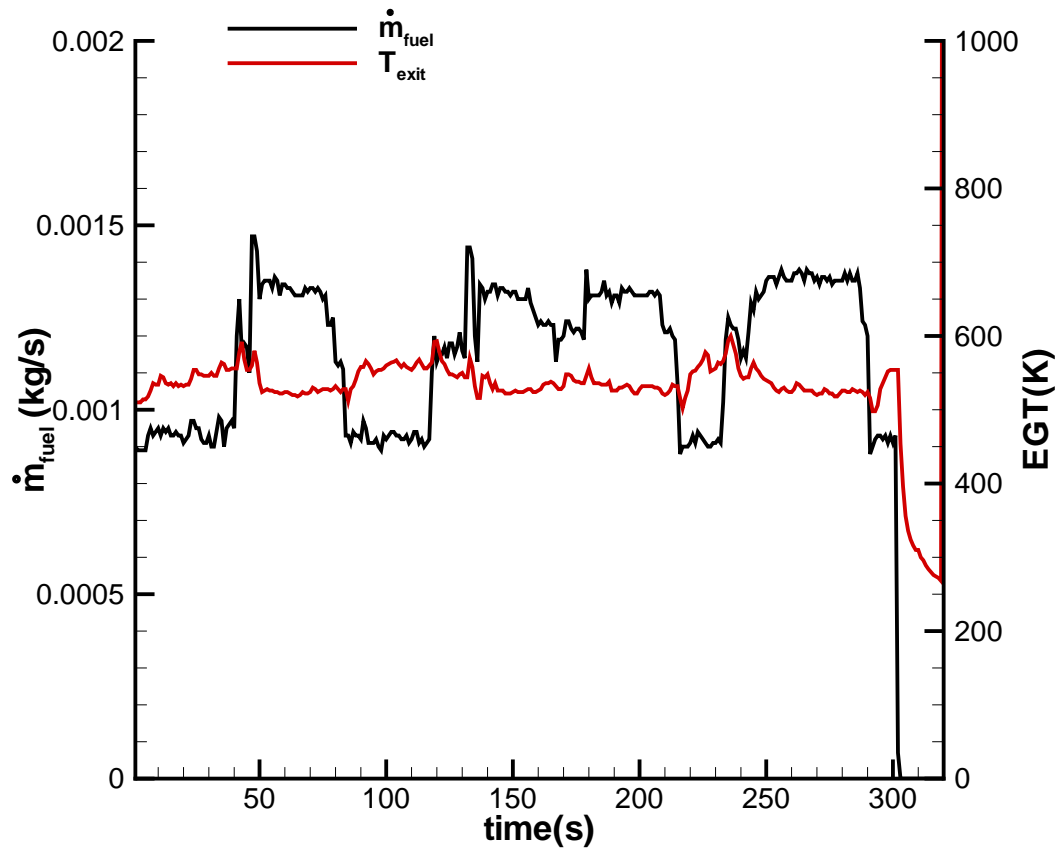


Figure 4.6: The response of engine exhaust gas temperature to quasi-step inputs in the fuel mass flow rate.

aero-thermal turbojet engine model are investigated by applying the same fuel scheduling scenario applied in the experiment to the model. The aero-thermal engine model of SimJet could not be developed due to the non-availability of the compressor map that belongs to Simjet.

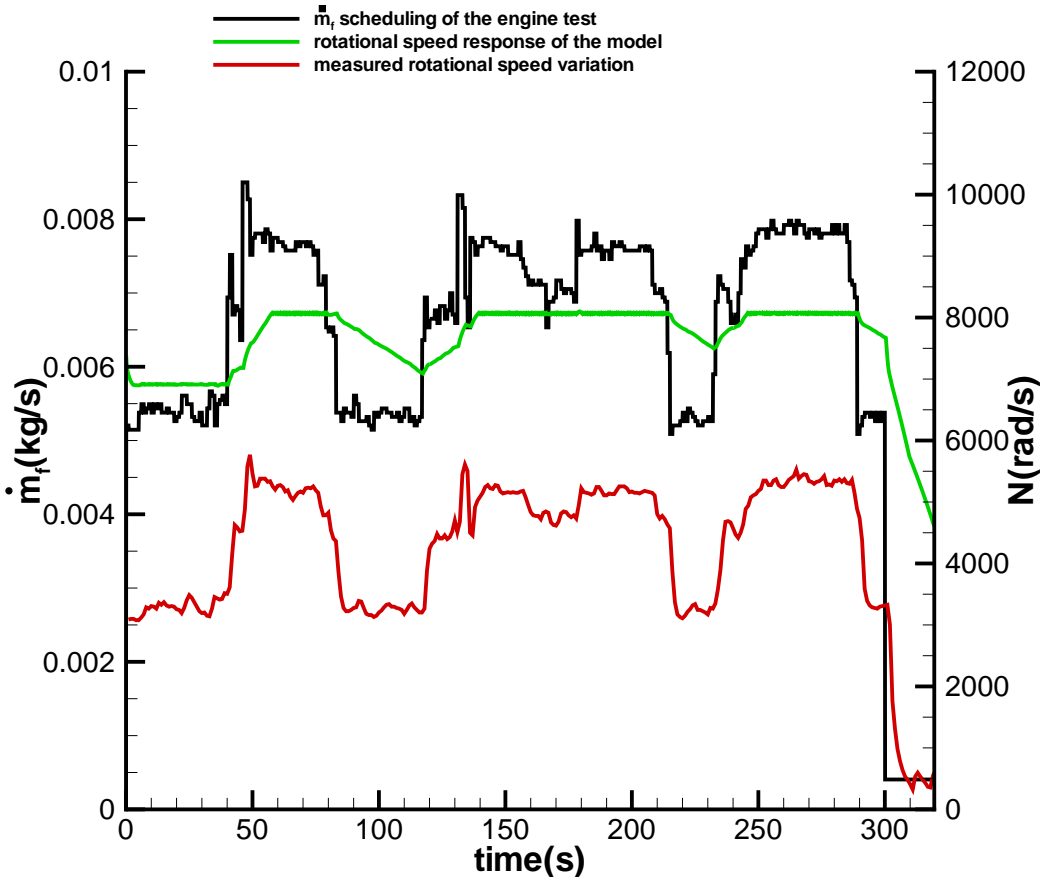


Figure 4.7: The response of engine model rotational speed to quasi-step inputs in the fuel mass flow rate.

As a first step, the fuel flow rate data measured during the experiment are normalized. These normalized fuel flow rate data are multiplied by the fuel flow rate value of the small turbojet engine which is the on-design fuel flow rate value. In order to observe the engine rotational speed and thrust responses of the small turbojet engine simulation model, this fuel flow rate data set which shows the same trend with the data set measures during experiment are inputted to the small turbojet engine simulation code. The response of engine rotational speed,

thrust and exhaust gas temperature are plotted and presented as in Figure 4.7, Figure 4.8 and Figure 4.9.

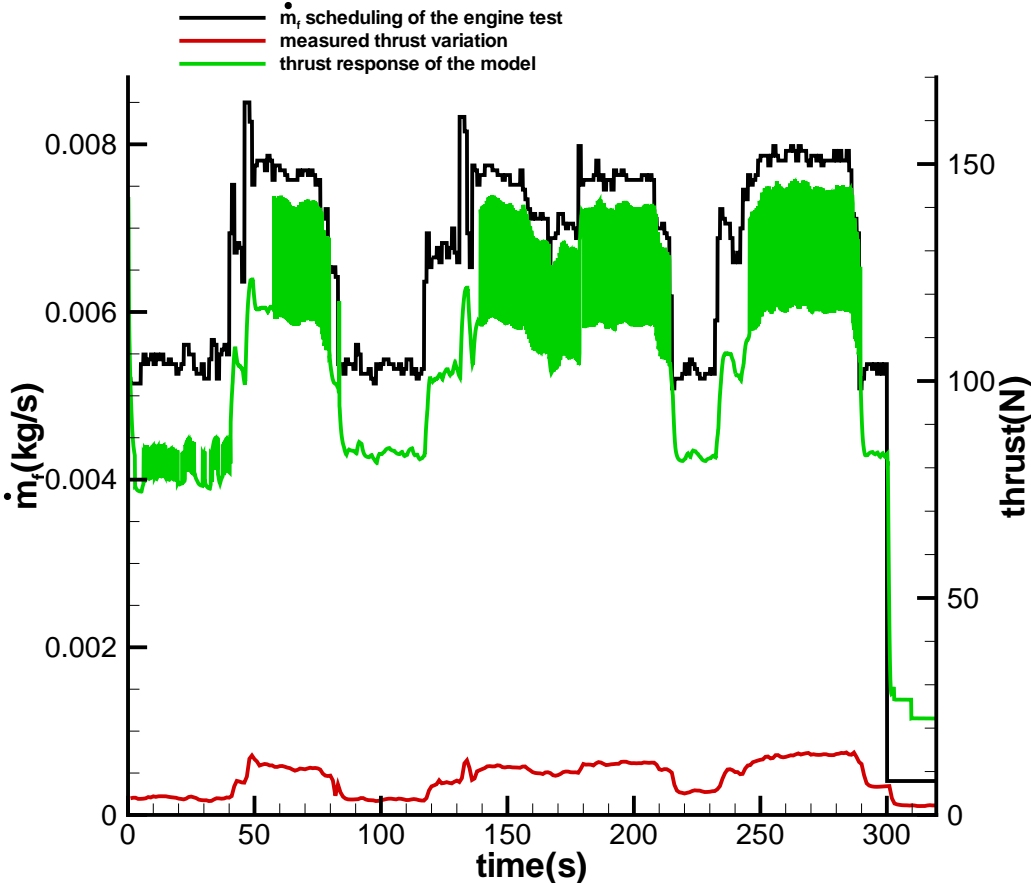


Figure 4.8: The thrust response of the engine model to quasi-step inputs in the fuel mass flow rate.

As shown in Figure 4.7, engine rotational speed response of the small turbo-jet model is consistent with the fuel flow rate input. When the fuel flow rate input is increased or decreased, rotational speed value shows the same trend. Because of the lagging response of the rotational speed which may be due to incorrect inertia value, the exact fuel flow rate input could not be captured but the expected increasing and decreasing trend of the rotational speed is obtained. As mentioned before, an investigation is performed in order to improve the response of rotational speed and avoid lag of rotational speed response in time. As a result of this investigation a new engine inertia value is used in the model.

This modification improved the rotational speed input but a lag in time still exists. The root cause of this lagging rotational speed response is found out to be due to the characteristic of existing shaft dynamics modeling equation. A new modeling of shaft dynamics may be performed by taking the turbomachinery concept into account by using Euler turbomachinery equation.

As shown in Figure 4.8, the thrust response of the small turbojet engine model follows closely the fuel flow rate input. In the areas where fuel flow rate input varies rapidly, the model responds to this varying input in an oscillating fashion. When simulation study result and validation study result are compared, the response of engine model thrust is fairly close to the response of real engine thrust.

In Figure 4.9, the Exhaust Gas Temperature(EGT) response of the small turbojet engine model is presented. The exhaust gas temperature value follows the fuel flow rate input and it responds quickly to the increasing and decreasing trends of the fuel flow rate. When it is compared with the experimental results of the SIMJET engine, it is observed that the exhaust gas temperature response of the real engine is varying in a narrow margin and presents a quasi-constant behaviour. As mentioned before, this behaviour can be explained by the action of the ECU which is a part of SimJet engine test facility. The ECU directly controls the fuel pump and adjusts the fuel flowrate value by using the exhaust gas temperature as feedback. This control algorithm tries to keep the exhaust gas temperature value in a margin in order to avoid an overspeed or possible engine damage. In the small turbojet engine model no control algorithm is implemented. Therefore the response of exhaust gas temperature of the model shows an expected trend.

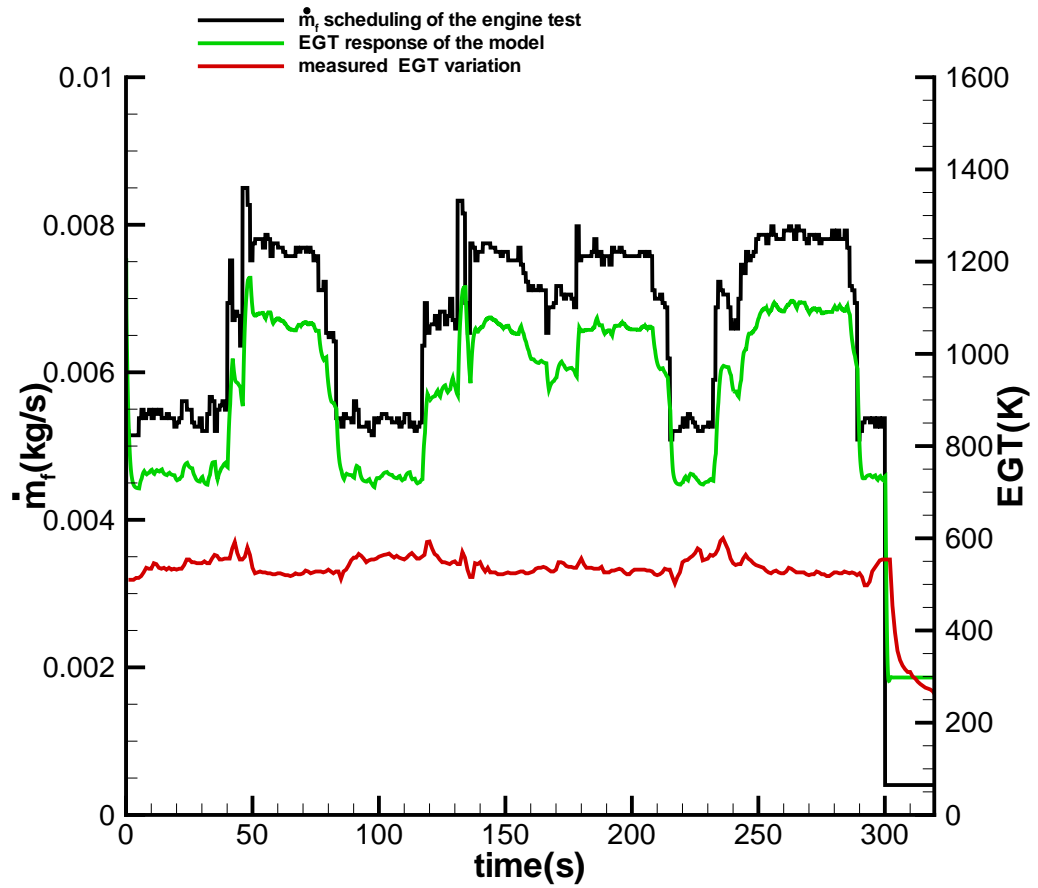


Figure 4.9: The exhaust gas temperature response of the engine model to quasi-step inputs in the fuel mass flow rate.

CHAPTER 5

TURBOSHAFT SIMULATIONS

5.1 Turboshift Engine Characteristics

Simulation of T800-LHT-800 turboshaft engine is performed as a second application of the aero-thermal transient engine model. T800-LHT-800 turboshaft engine, shown in Figure 5.1, is developed for the US Army by the Light Helicopter Turbine Engine Company (LHTEC), a partnership between Allison Engine Company and Allied Signal Engines. Some of Agusta A129 Mangusta helicopters, shown in Figure 5.2, are powered by T800-LHT-800 turboshaft engines.

T800-LHT-800 is a turboshaft engine with a two stage centrifugal compressor driven by a two stage axial turbine, and the load is driven by a two stage free power turbine. Air enters at the front of the engine through an annular duct that surrounds the engine output. At the front of the engine there is an integrated vaneless inlet particle separator. The engine features a very simple yet efficient two stage centrifugal compressor. Air from the first centrifugal compressor stage is turned 180 degrees to feed the eye of the second stage impeller. The second centrifugal compressor stage feeds the compressed airflow to an annular reverse flow, machined ring combustor. Combustion gas is turned 180 degrees before it is fed to the two stage axial gas producer turbine, which drives the compressor and the accessory geartrain. The first stage turbine is transpiration cooled for higher turbine inlet temperatures. The second stage is uncooled. The load is driven by a two stage axial free power turbine. The turbine turns a shaft which runs coaxially through the center of the gas producer shaft. Engine has an elec-

tronic fuel controller and governor and an electric starter and generator. Spare drive pads are provided for hydraulic pumps and other additional accessories. Engine control is fully electronic, using a state of the art FADEC system. The electronic control system provides N1 speed control, N2 governing, overspeed and overtemperature protection, surge control and acceleration limiting. [20]

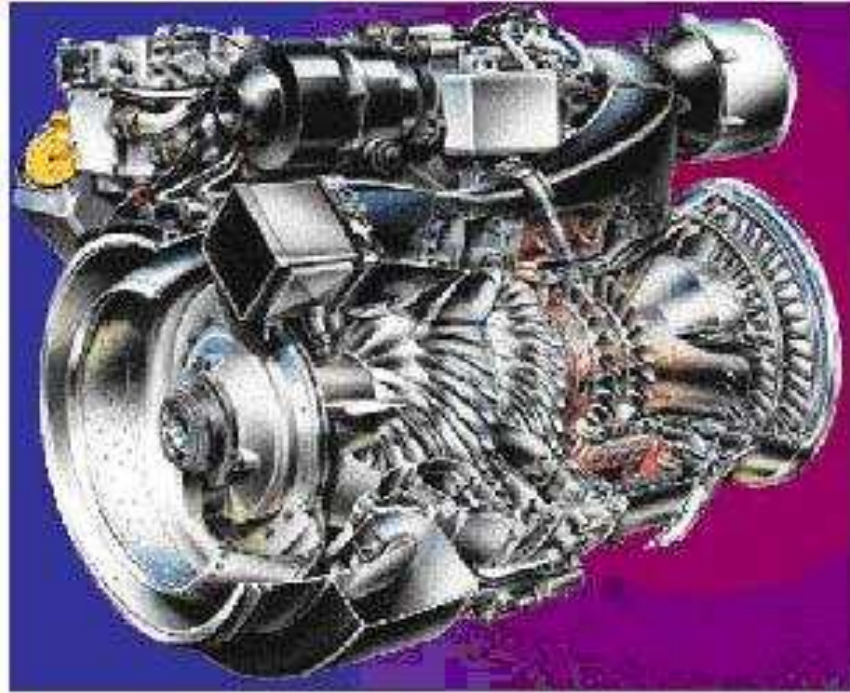


Figure 5.1: T800-LHT-800 Turboshaft Engine.

Design point characteristics of T800-LHT-800 turboshaft engine are given in Table 5.1. An on-design cycle analysis is performed following the methodology presented in [15], and outputs are used as the turboshaft reference point data and as inputs to the simulation code. Both the gas generator and the power turbines are assumed to be operating at choked flow conditions. The gas generator turbine inlet temperature is assumed to be 1700 K.

The problem of Hot-Gas Ingestion (HGI) is studied specifically as a part of this application. This problem is experienced in general by rotorcraft as well as VTOL or STOVL fixed-wing aircraft under hovering conditions in the proximity to the ground. Helicopters in particular are susceptible to HGI because while



Figure 5.2: Agusta A129 Mangusta Helicopter.

Table 5.1: Specifications of T800-LHT-800 turboshaft engine [17].

Parameter	Value	Unit
\dot{m}_{air} (<i>massflowrate</i>)	3.3	kg/s
Π_c	14:1	
N_{GG} (<i>gasgeneratorrotationalspeed</i>)	43800	rpm
P_{pt} (<i>ratedpower</i>)	1334	shp
<i>Diameter</i>	546.24	mm
<i>Length</i>	858	mm
<i>Weight</i>	315	lbs

hovering in ground effect, exhaust gases that are contained within the rotor downwash can be ingested by the engine. HGI may also occur when exhaust gases at high temperatures due to rocket launching or gun firing directly enter the engine causing a degradation in engine power levels. The HGI study in this thesis is preferred specifically for observing the potential of the gas turbine model in simulating real world operational scenarios.

During HGI, temperature distortion at the engine inlet is the principal factor affecting the performance and stability limits of the engine. In an experimental study by [10], in which both the steady state and transient response of the compressor of a small turboshaft engine to inlet temperature distortion is investigated, it has shown that rapid temperature rise at engine inlet may lead to compressor surge. Also, as indicated in [11], under steady state operating conditions, a 1°C engine inlet air temperature increase may reduce the power available approximately by 1%. In [12], simulation results for the hydromechanical fuel control on the Lycoming T53 turboshaft engine in a rocket launch HGI scenario on an AH-1 Cobra helicopter are presented. HGI is also experienced by fixed-wing STOVL aircraft during the descent phase of landing, or while on the ground. The hot exhaust gases from downwards pointing nozzles can be re-ingested into the engine intakes, causing power degradation or reduced engine surge margin ([13], [14]). Surge margin is the margin of safety between the normal operating point of the compressor and the stability limit.

In order to perform the simulation of T800-LHT-800, the compressor map of the

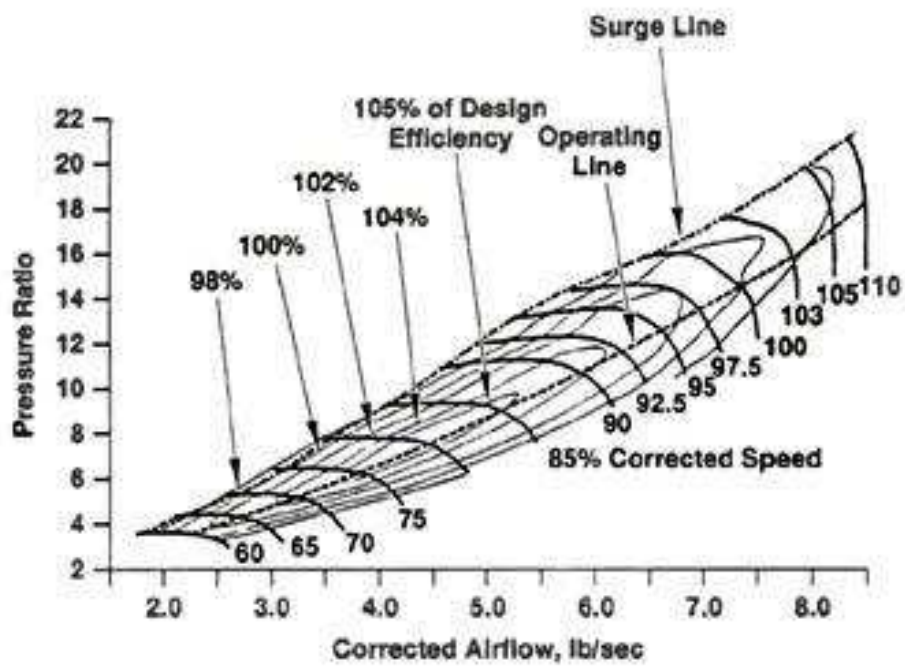


Figure 5.3: Compressor map of T800-LHT-800 as given in [17].

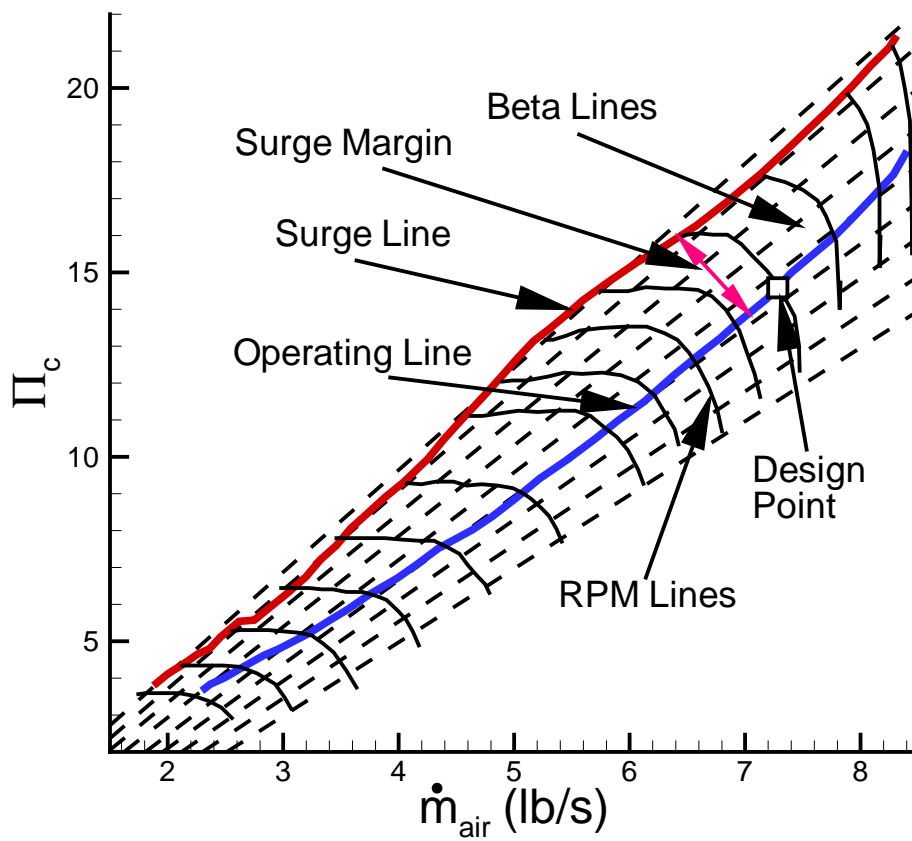


Figure 5.4: Digitized version of T800-LHT-800 compressor map that is used to generate the look-up tables.

turboshaft engine, as given in [17], is loaded to the simulation code in the form of look-up tables. For this simulation case, β -lines are generated as straight lines, which do not intersect each other and are equally spaced. This is a particular choice which is made for this study for simplification purposes. Previous studies have used parabolae for this purpose (e.g. [16]). Figures 5.3 and Figure 5.4 show the original as well as the digitized compressor maps, respectively, with β -lines superimposed.

5.2 Results

The results of the simulation of the transient response of T800-LHT-800 turboshaft engine to HGI are presented. The simulation scenarios are selected specifically to observe the variations in the surge margin and the transient behaviour of the engine near the surge line due to HGI. Two different temperature distortion scenarios are introduced at the engine inlet, both being step changes in the inlet temperature levels but at different magnitudes.

In the first scenario, engine inlet temperature stays at its reference level for 30 seconds and then increases to a value 5.3% higher than its reference level and stays at that value till $t=60s$, i.e. the end of the simulation. For the second scenario again a step change is applied with a higher temperature increase to a value 15% higher than the reference. The temperature distortion limits are decided after executing the simulation code at different distortion levels, and it was observed that any inlet temperature distortion higher than 15% resulted in a compressor surge due to the reduction in the inlet mass flow rate levels. In real world events, it has been observed both from experiments as well as flight test data that the inlet temperature distortion levels could be as high as 30% ([10], [12]).

This reduction in the inlet mass flow rate due to the temperature distortion is calculated assuming the gas is a perfect gas, the inlet pressure changes are negligible (also confirmed from the data presented in [12]) and using the equation

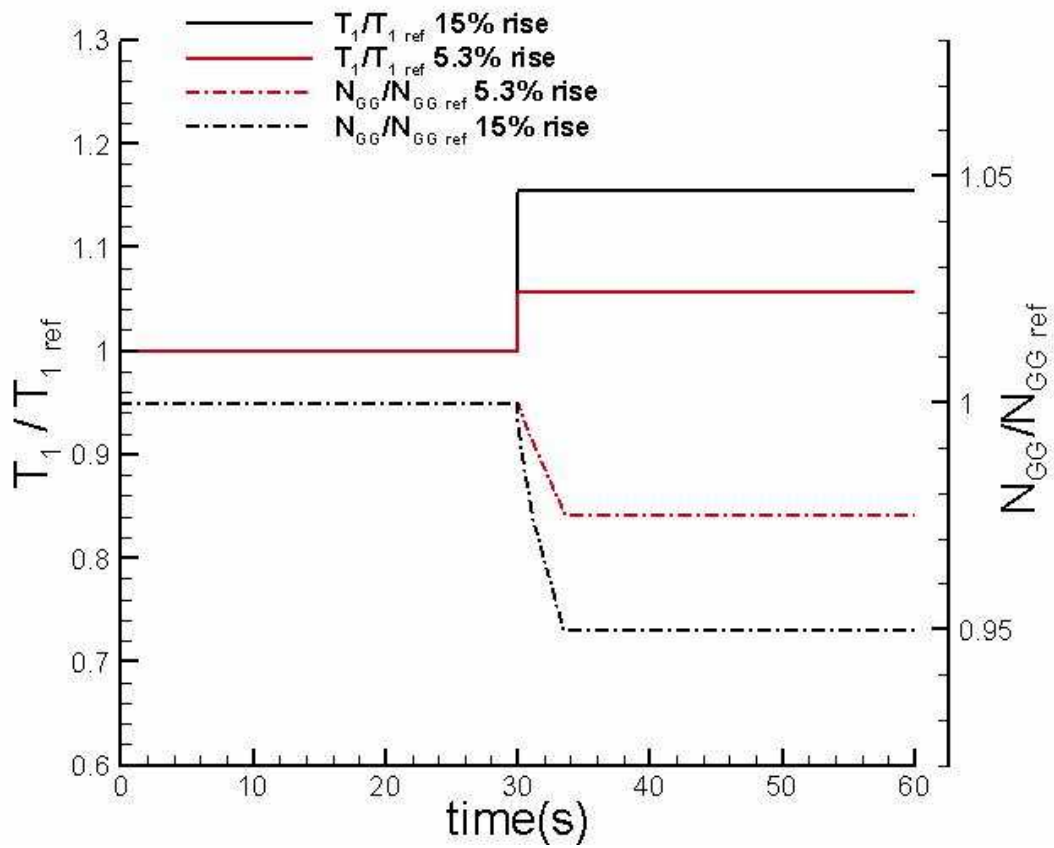


Figure 5.5: The response of T800-LHT-800 engine gas generator speed to 5.3% and 15% increase in engine inlet temperature.

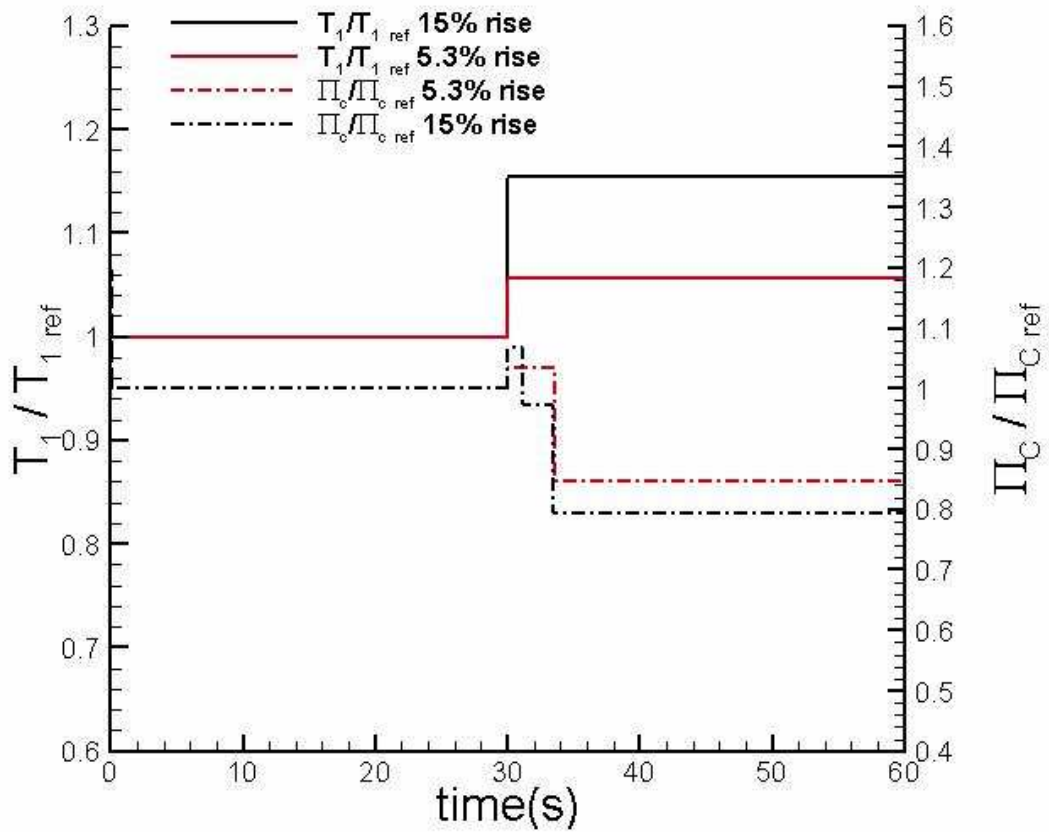


Figure 5.6: The response of T800-LHT-800 engine compressor pressure ratio to 5.3% and 15% increase in engine inlet temperature.

of state for an ideal gas,

$$\dot{m}_{air,HGI} = \dot{m}_{air} \times \sqrt{\frac{T_1}{T_{1,HGI}}}. \quad (5.1)$$

Figure 5.5, Figure 5.6 and Figure 5.7 show the variations of the gas generator speed, compressor pressure ratio and power output for these two scenarios, respectively. These are open-loop simulations performed at constant fuel flow rate. All values are normalized against their original levels. During the first 30 seconds as the inlet temperature stays at its reference level, all three parameters stay at their corresponding reference levels, showing that the engine is operating at steady state conditions near the design point.

When a 5.3% step input is applied to the inlet temperature, the gas generator speed decreases to a value about 2.5% lower than its reference value in about 4 seconds and rests at that value till t=60 s. In the second case, when a 15% step input is applied to the inlet temperature, the reduction is now about 5% in 4 seconds showing almost a two times faster deceleration in the gas generator speed.

As to the compressor pressure ratio shown in Figure 5.6, when a 5.3% step input is applied to inlet temperature, it first increases to a value 3.3% higher than its reference value and after 4 seconds decreases to a value 15% lower than its reference value and rests at that value till t=60s. When a 15% step input is applied to inlet temperature, compressor pressure ratio for a short time interval increases to a value 7% higher than its reference value and then quickly gets reduced to a value 21% lower than its reference value in about 4 seconds. The step-like changes in the compressor pressure ratio is mainly due to the fact that the data is being read as discrete values from the look-up tables.

The power output (available) shows an interesting trend as shown in Figure 5.7. A 5.3% step change in the inlet temperature first causes a sudden decrease in the power output level about 3.2% followed by an increase to a level of 1.5% lower than its original value and a decrease back to a level of 3% lower than the original value. This variation lasts about 6 seconds after which it keeps the

same until $t=60s$.

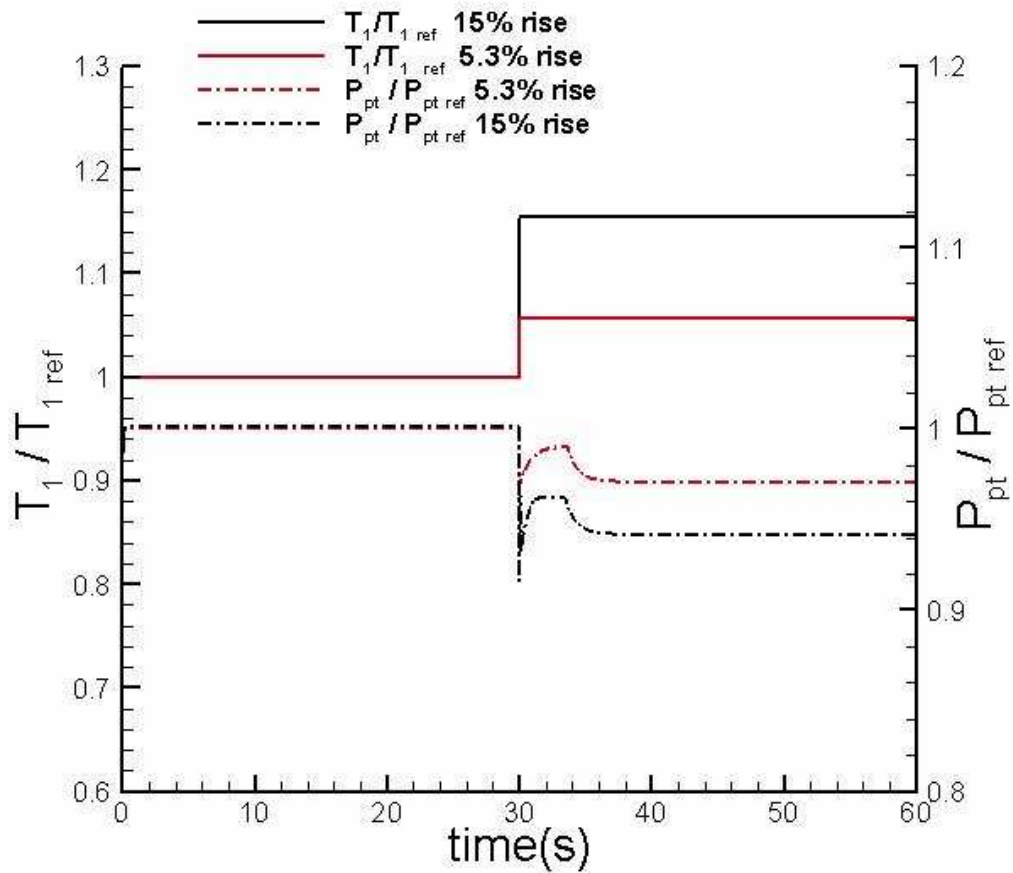


Figure 5.7: The response of T800-LHT-800 engine power output to 5.3% and 15% increase in engine inlet temperature.

In the second scenario, i.e. when a 15% step input is applied to inlet temperature, the power output variations are similar but higher reductions in power levels are observed. The power output suddenly decreases to a value that is 8% lower, increases to a value 4% lower than its reference value and decreases back to a value 6% lower than the original.

This behaviour can be explained as follows:

As soon as HGI occurs, the mass flow rate suddenly decreases which results in an instantaneous loss of power. However as the engine operates on the same rpm line at the time of ingestion, compressor pressure ratio gets increased and engine keeps operating with that increased pressure ratio for a few seconds. Increased

pressure ratio value results in an increase in the compressor exit temperature. The gas generator turbine inlet temperature and power turbine inlet temperature are increased subsequently which causes slight increase of power for a few seconds before the pressure ratio decreases to a steady state value. Then the engine starts to operate at a smaller rpm line with a relatively low pressure ratio and reaches to a steady-state condition.

Figure 5.8 shows the effect of HGI on the reduction of the surge margin of the compressor. When a 5.3% temperature rise is experienced at the inlet, engine's operating point jumps to a point closer to the surge line and then descends to a point on the operating line but at a lower rpm value. It stays at this point until the end of the HGI simulation time period. If the temperature distortion is more severe such as 15%, the operating point jumps to a position very close to the surge line and then relaxes back to a point just under the operating line. As a result, the increase in the probability of having an engine surge at higher inlet temperature distortion levels is successfully captured by the dynamic model.

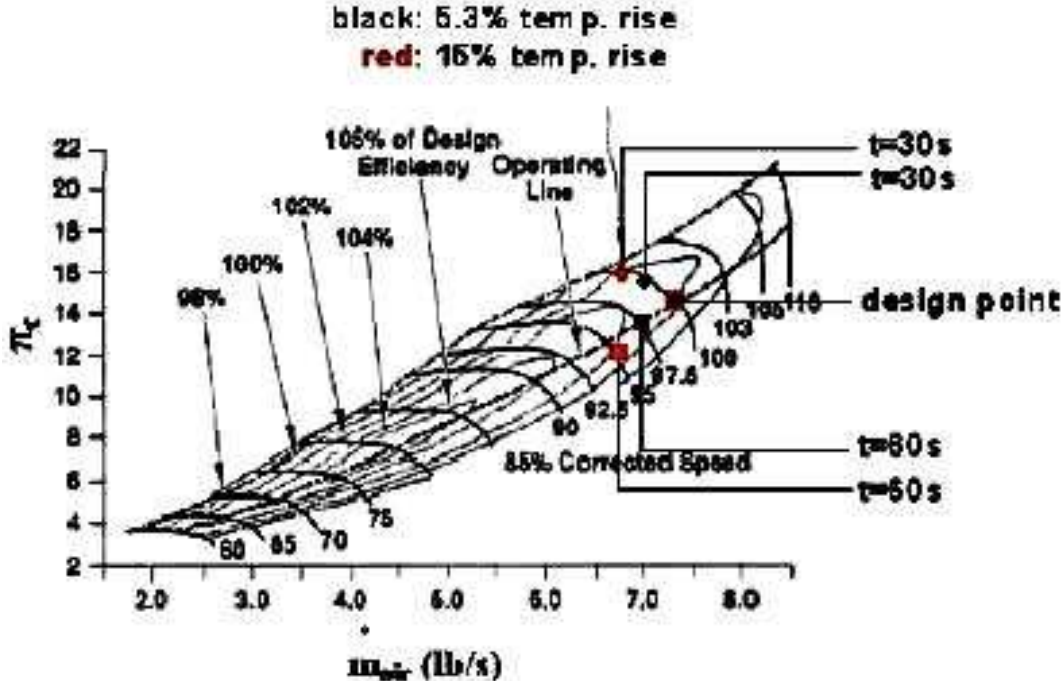


Figure 5.8: Effect of HGI on the surge margin for two different inlet temperature distortions.

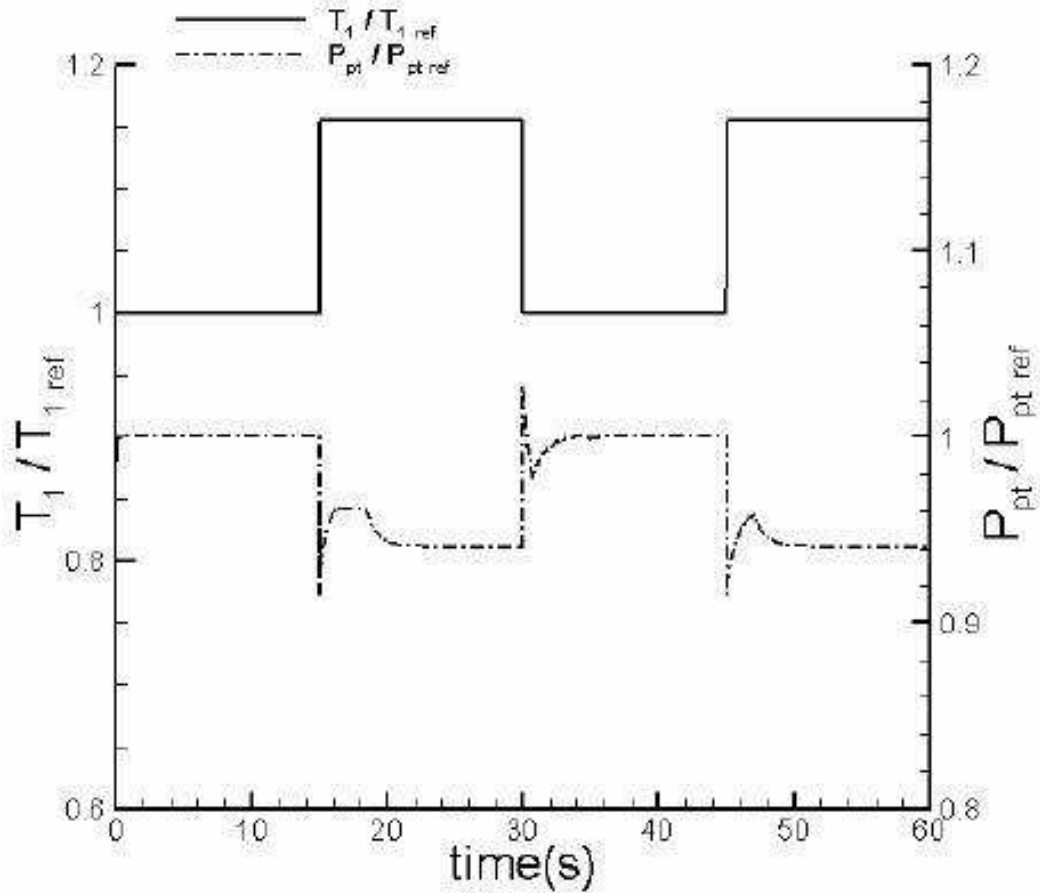


Figure 5.9: The response of T800-LHT-800 engine power output to double step input of temperature rise at engine inlet. Hot gas ingestion simulation scenario II.

Figure 5.9 shows the results of an additional HGI scenario which is a double step change with a 15% increase in engine inlet temperature. The response of the power output is plotted over a 60 second period composed of 4 legs. For the first leg of 15 seconds, power value rests at its reference value as the inlet temperature stays at its reference level. As the temperature increases to a value 15% higher than its reference value, power output shows an oscillating behaviour for 4 seconds and then stabilizes at a value 6% lower than its reference value and then rests at that value till $t=30s$, similar to the results presented in Figure 5.7. When the inlet temperature comes back to its reference value (3rd leg), the power level first overshoots then undershoots within about 1 second and then slowly stabilizes at its reference value. During the fourth leg of the scenario, the

power output responds in a similar manner as in the second leg of the scenario, however some differences in the transient response are clearly evident.

These differences may be explained as follows: During the 1st HGI input which is applied for 15 seconds, N_{GG} value is decreased to a specific value. When inlet conditions return back to the reference values and rest there for another 15 seconds, N_{GG} does not reach to the original value but reaches to a value between the N_{GG} values at legs 1 and 2. This causes an increase in the pressure ratio value at the time of the 2nd HGI, which is different from the one at the time of the 1st HGI event. This variation in pressure ratio is the main reason behind the power turbine output levels at legs 2 and 4.

5.3 A Sample RPM Controller

As a part of this study, a simple proportional feedback controller is implemented in order to keep the gas generator rotational speed constant in the event of HGI.

In the open loop case, initial values of PT load and PT speeds are input parameters as well as the atmospheric temperature, pressure and the Mach number. Fuel flow rate is constant in the open loop case. In the closed loop case, fuel flow rate is the control parameter and gas generator turbine rotational speed is tried to be kept constant.

Figure 5.10 shows a comparison of the gas generator speed response with and without a control strategy to a 15% increase in the engine inlet temperature. As the inlet temperature is increased, the controller starts to increase the fuel flow rate, while keeping the fuel-to-air ratio which is calculated just after the experience of temperature distortion at engine inlet constant, as shown in Figure 5.11, and keeps the rotational speed constant, compensating for the reduction in the air mass flow rate due to HGI. Nevertheless, the performance of this simple proportional control system is really not very high. When the controller is applied, high amplitude oscillations start to occur in the compressor pressure ratio, which is due to the inadequate representation of the compressor map through

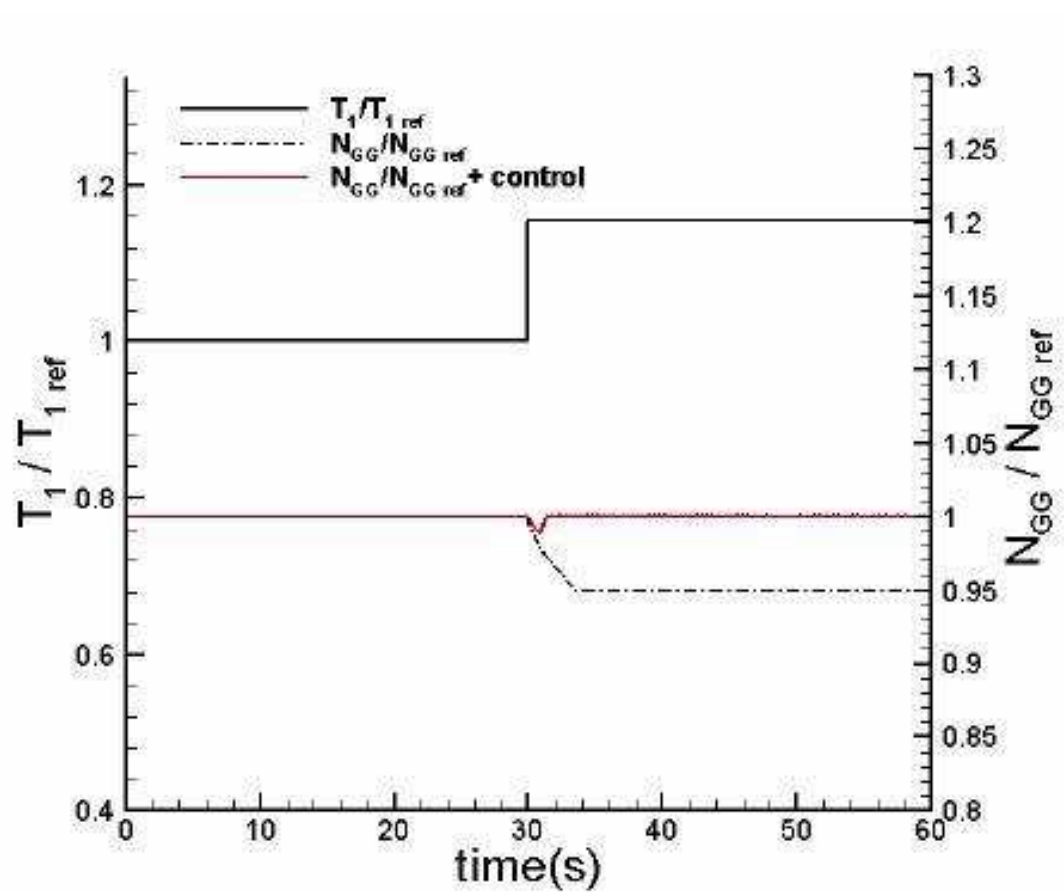


Figure 5.10: The response of T800-LHT-800 engine gas generator speed with and without the control system.

the look-up tables. Replacing look-up tables which represents the compressor map by a neural network algorithm can be a solution to this problem.

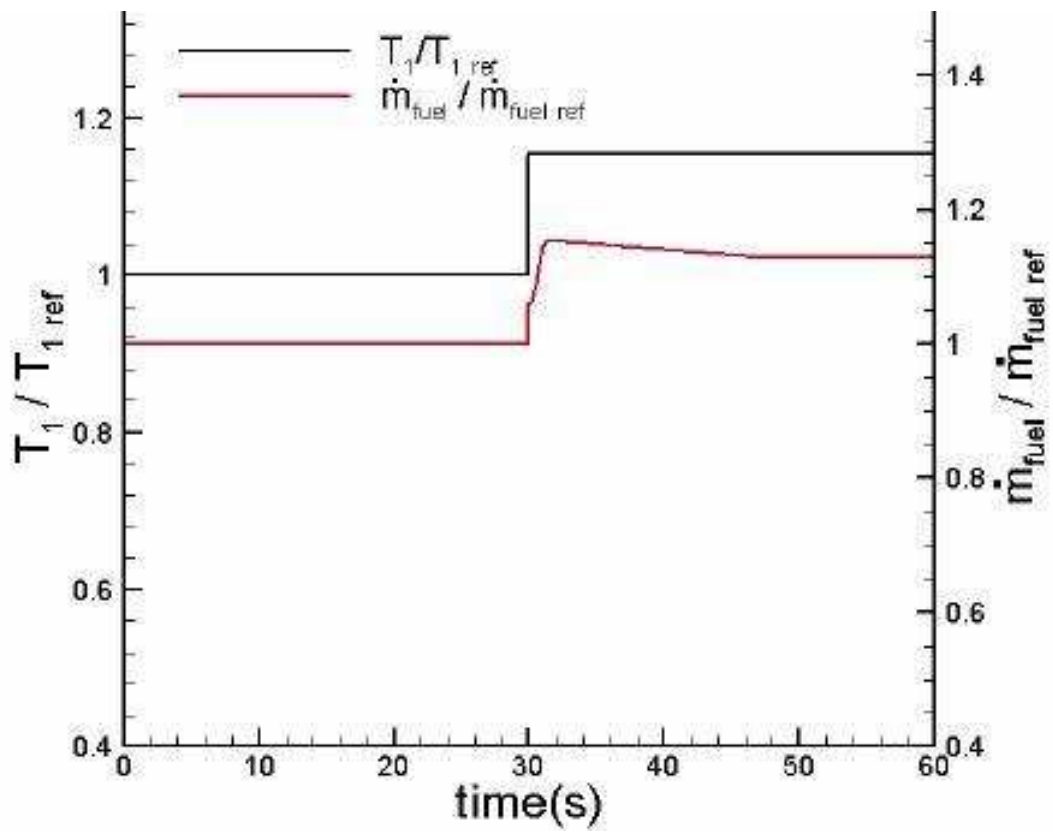


Figure 5.11: The variation of the control parameter fuel flow rate.

CHAPTER 6

CONCLUSIONS AND FUTURE WORK

6.1 CONCLUSIONS

A generic aerothermal transient gas turbine engine model is structured and a simulation code which is based on this aerothermal model is developed. Simulation of a small turbojet engine by applying different fuel scheduling scenarios and a hot gas ingestion scenario for a turboshaft engine are performed.

The aerothermal gas turbine engine model is based on a mathematical model which consists of the governing equations representing the aero-thermodynamic process of the each engine component. The algorithm of the mathematical model is composed of a set of differential equations and a set of non-linear algebraic equations representing each turbojet engine component. At each time step, ordinary differential equations are integrated by a first-order Euler scheme and a set of algebraic equations are solved by forward substitution.

The compressor map data is loaded to the simulation code by using the β -lines technique. By generating β -lines on the compressor map, a grid is formed which provides discrete points. The data from those points are used in order to prepare the look up tables. Two separate look up tables are formed, which allow the code to read the pressure ratio and the mass flow rate knowing the β -lines index and the speed value. The efficiency is assumed to be constant in this study and a third look-up table is not used for efficiency calculations.

In the first simulation study, an aero-thermal model of a small turbojet engine

with no bleed and no turbine cooling is developed in order to simulate in real-time the critical transients that it may suffer at off-design operating conditions. Results of the engine response are presented for two sample scenarios that simulates different fuel scheduling applications. Simulation results show that the code captures the transient behaviour of a turbojet engine under various loading and operating conditions.

In the second simulation, different Hot Gas Ingestion (HGI) scenarios are performed using the generic simulation code based on an aero-thermal model of T800-LHT-800 turboshaft engine. Simulation results show that the code has the potential to correctly capture the transient behaviour of a turboshaft engine under various HGI conditions, such as the reduction in the gas generator speed and the power levels as well as the decrease in the compressor surge margin. The code can also be used for developing engine control algorithms as well as health monitoring systems, and can easily be integrated in to a flight simulator after appropriate validation studies, increasing the level of fidelity of the simulation system. As a part of this study, a simple proportional feedback controller is also implemented in order to keep the gas generator rotational speed constant in the event of HGI. As the inlet temperature is increased, the controller starts to increase the fuel flow rate, while keeping the fuel-to-air ratio constant and keeps the rpm constant, compensating for the reduction in the air mass flow rate due to HGI. Nevertheless, the performance of this simple proportional control system is really not very high. When the controller is applied, high amplitude oscillations start to occur in the compressor pressure ratio, which which are known to be due to the inadequate representation of the compressor map through the look-up tables. In order to solve this problem, look up tables introduced by β -lines techniques may be improved and a study may be performed to replace them with a neural network based algorithm in future studies.

A validation study is performed for aero-thermal turbojet engine model. In order to use in the validation study of the generic gas turbine engine simulation code, a system identification study for a small turbojet engine is performed by measuring the transient response of the engine to a variable rotational speed scenario. The fuel flow rate input which corresponds to the rotational speed

scenario is recorded. Engine rotational speed, engine thrust and exhaust gas temperature values are measured and the results are plotted. Same fuel flow rate scenario are input to the simulation code and the responses engine rotational speed, thrust and exhaust gas temperature values are plotted in order to compare with experimental results. As a result of the comparison, it is concluded that the aero-thermal model responds closely to a real gas turbine engine but needs some further improvements.

6.2 FUTURE WORK

As a future work, in order to avoid the lag in rotational speed response of the engine model, shaft dynamics may be remodeled by taking the turbomachinery concept into consideration. Shaft dynamics can be modeled using Euler Turbomachinery equation and engine rotational speed can be calculated through this equation.

In addition to this, in order to damp out some of the oscillations in response plots, a fine beta line grid may be structured on the compressor map and more data from the map can be recorded to look up tables.

As a second solution, in order to damp out the oscillations in response plots, look up tables may be replaced by a neural network algorithm which defines continuous functions.

Finally, there may also be a physical reason behind the oscillations induced in response graphs. As a future work, this concept may be investigated by using the methodologies given in [22].

REFERENCES

- [1] Camporeale, S.M. ; Fortunato, B.; Mastrovito, M.; " A Modular Code For Real-Time Dynamic Simulation of Gas Turbines in Simulink", ASME Journal of Engineering for Gas Turbines and Power, 2006, Vol. 128, pp.506-517.
- [2] Sampath, S. ; Gulati, A.; Singh, R.; " Fault Diagnostics Using Genetic Algorithm for Advanced Cycle Gas Turbine ", Proceedings of ASME TURBO EXPO 2002, June 3-6, 2002, Amsterdam, Netherlands
- [3] Kirkman, M ; " The Use of Simulation in the Design of Modern Gas Turbine Control Systems ", Integrated Systems in Aerospace (Digest No: 1997/015), IEE Colloquium on 18 Feb 1997
- [4] Walsh, P.P.; Fletcher, P. ; "Gas Turbine Performance", Blackwell Science, Oxford, 1998.
- [5] Lichtsinder, M. ; Levy, Y. ; "Jet Engine Model For Control and Real-Time Simulations", ASME Journal of Engineering for Gas Turbines and Power, 2006, Vol. 128, pp. 745-753.
- [6] Camporeale, S.M. ; Fortunato, B.; Mastrovito, M.; " A High Fidelity Real-Time Simulation Code of Gas Turbine Dynamics For Control Applications", ASME paper, 2002, GT-2002-30039.
- [7] Bozzi, L; Crosa, G.; Trucco, A.; "Simplified Block Diagram of Twin Shaft Gas Turbines", Proceedings of ASME Turbo Expo 2003, Power for Land, Sea and Air , 2003
- [8] Al-Hamdan, Q.Z.; Ebaid, M.S.Y.;"Modelling and Simulation of a Gas Turbine Engine for Power Generation", " , ASME Journal of Engineering for Gas Turbines and Power, 2006, Vol. 128, pp. 302-311.
- [9] Korakianitis, T.; Hochstein, J.I.; Zou, D.; "Prediction of the Transient Thermodynamic Response of a Closed-Cycle Regenerative Gas Turbine" ASME Journal of Engineering for Gas Turbines and Power, 2005,Vol. 127, pp.57-64.
- [10] Biesiadny , Thomas J.; Klann, Gary A.; Little, Jeffery K.; "Response of a Small-Turboshaft-Engine Compression System to Inlet Temperature Distortion" NASA Technical Memorandum 83765; USA AVSCOM Technical Report 84-C-13; 1986
- [11] Jackson, M. E., House, R. L., 1981, "Exhaust Gas Reingestion during Hover In-Ground-Effect," Proceedings of 37th Annual Forum of the American Helicopter Society, New Orleans, Louisiana, May 1981.

- [12] Tokarski, F.; Desai, M.; Books, M.; Zagranski, R.; "Hot Gas Ingestion Effects on Fuel Control Surge Recovery and AH-1 Rotor Drive Train Torque Spikes", NASA Contractor Report 191047, Army Research Laboratory, Contractor Report ARL-CR-13, 1994
- [13] Richardson, G. A.; Dawes, W. N.; Savill, A. M.; "CFD Analysis of Hot Gas Ingestion Mechanisms for the Vertical Descent Phase of a Harrier Aircraft", Proceedings of ASME: Turbo Expo May 2006, Barcelona, Spain, GT2006-90766.
- [14] Chaderjian, Neal M.; Pandya Ö, Shishir A.; Ahmad, Jasim U.; Murman, and Scott M.; "Progress Toward Generation of a Navier-Stokes Database for a Harrier in Ground Effect" Biennial International Powered Lift Conference and Exhibit 5-7 November 2002, Williamsburg, Virginia.
- [15] Mattingly, J.D.; Heiser, W.H.; Pratt, D.T.; "Aircraft Engine Design 2nd Edition", AIAA Education Series, 2002.
- [16] Kurzke, Joachim; "How To Get Component Maps For Aircraft Gas Turbine Performance Calculations", "International Gas Turbine and Aeroengine Congress and Exhibition", 1996.
- [17] Palmer, D. L.; Waterman W. F.;"Design and Development of an Advanced Two Stage Compressor"; Journal of Turbomachinery; April 1995.
- [18] <http://www.festo.com/INetDomino/coorpsites/en/cfa07fe08d8f44f4c1256b4100368542.htm>
- [19] SimJet Miniature Turbojet Engine Owner's Manual
- [20] <http://www.turbokart.com/aboutt800.htm>
- [21] Kaya, H.; Uçan,K.; Başlamışlı, U.; Koç, Y.; AE438 Term Project; June 2007
- [22] Greitzer, E. M.; Tan, C. S.; Graf M. B.; "Internal Flow Concepts and Applications", Cambridge University Press, 2004